This article was downloaded by:[EBSCOHost EJS Content Distribution]
On: 25 March 2008
Access Details: [subscription number 768320842]
Publisher: Taylor & Francis
Informa Ltd Registered in England and Wales Registered Number: 1072954
Registered office: Mortimer House, 37-41 Mortimer Street, London W1T 3JH, UK

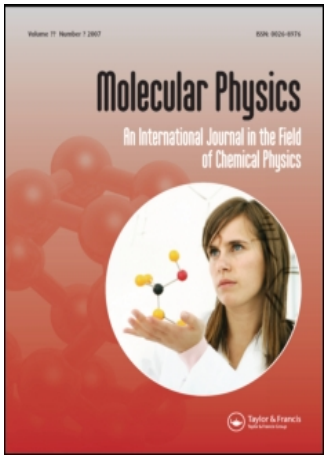

Molecular Physics
An International Journal in the Field of Chemical Physics
Publication details, including instructions for authors and subscription information:
http://www.informaworld.com/smpp/title~content=t713395160

Derivation of a general fluid equation of state based on the quasiGaussian entropy theory: application to the Lennard-Jones fluid

A. Amadei; M. E. F. Apol; G. Chillemi; H. J. C. Berendsen; A. Di Nola

Online Publication Date: 20 May 1999
To cite this Article: Amadei, A., Apol, M. E. F., Chillemi, G., Berendsen, H. J. C. and Nola, A. Di (1999) 'Derivation of a general fluid equation of state based on the quasiGaussian entropy theory: application to the Lennard-Jones fluid', Molecular Physics, 96:10, 1469 - 1490
To link to this article: DOI: 10.1080/002689799164423
URL: http://dx.doi.org/10.1080/002689799164423

PLEASE SCROLL DOWN FOR ARTICLE

Full terms and conditions of use: http://www.informaworld.com/terms-and-conditions-of-access.pdf

This article maybe used for research, teaching and private study purposes. Any substantial or systematic reproduction, re-distribution, re-selling, loan or sub-licensing, systematic supply or distribution in any form to anyone is expressly forbidden.

The publisher does not give any warranty express or implied or make any representation that the contents will be complete or accurate or up to date. The accuracy of any instructions, formulae and drug doses should be independently verified with primary sources. The publisher shall not be liable for any loss, actions, claims, proceedings, demand or costs or damages whatsoever or howsoever caused arising directly or indirectly in connection with or arising out of the use of this material.

MOLECULAR PHYSICS, 1999, VOL. 96, NO. 10, 1469–1490

Downloaded By: [EBSCOHost EJS Content Distribution] At: 14:09 25 March 2008

Derivation of a general fluid equation of state based on the quasi-Gaussian entropy theory: application to the Lennard-Jones fluid

A. AMADEI[1]*, M. E. F. APOL[1], G. CHILLEMI[2], H. J. C. BERENDSEN[3] and A. DI NOLA[1]

[1]Department of Chemistry, University of Rome 'La Sapienza', P.le A. Moro 5, 00185, Rome, Italy

[2] Inter-University Computing Consortium (CASPUR), University of Rome 'La Sapienza', P.le A. Moro 5, 00185, Rome, Italy

[3] Groningen Biomolecular Sciences and Biotechnology Institute (GBB), Department of Biophysical Chemistry, University of Groningen, Nijenborgh 4, 9747 AG Groningen, The Netherlands

(*Received 22 June 1998; revised version accepted 16 November 1998*)

In this article we present an equation of state for fluids, based on the quasi-Gaussian entropy theory. The temperature dependence along isochores is described by a confined Gamma state, previously introduced, combined with a simple perturbation term. The 11 parameters occurring in the free energy and pressure expressions along the isochores are obtained from molecular dynamics simulation data. The equation of state has been parametrized for the Lennard-Jones fluid in the (reduced) density range 0–1.0 and (reduced) temperature range 1.0–20.0 using (partly new) NVT molecular dynamics simulation data. An excellent agreement for both energy and pressure was obtained. To test the ability to extrapolate to unknown state points, the parametrization was also performed on a smaller set of data in the temperature range 1.0–6.0. The results in the two cases are remarkably close, even in the high temperature range, and are often almost indistinguishable, in contrast to a pure empirical equation of state, like for example the modified Benedict–Webb–Rubin equation. The coexistence line agrees in general very well with Gibbs ensemble and NpT simulation results, and only very close to the critical point there are deviations. Our estimate of the critical point for both parametrizations is somewhat different from the best estimate based on Gibbs ensemble simulations, but is in excellent agreement with other estimates based on NVT simulations and integral equations.

1. Introduction

Equations of state of fluids are of immense practical industrial importance. In practically all branches of chemical technology and materials science (oil refinery, gas and liquid separation, synthesis, polymerization, material design, etc.), detailed knowledge of equations of state (EOS) is mandatory.

It is common practice to model the phase behaviour of fluids and fluid mixtures with empirical or semi-empirical models. Up to now the equations of state most frequently used are empirical modifications of the van der Waals EOS, like the Soave–Redlich–Kwong and the Peng–Robinson equation [1]. These equations are satisfactory for simple apolar systems, but for more complex systems they only give acceptable results if many adjustable parameters are used. Another type of empirical EOS, the modified Benedict–Webb–Rubin (MBWR) equation, has been applied rather successfully to describe the pVT surface of, for example, air, para hydrogen, nitrogen, oxygen [2] and methane [3].

For the Lennard-Jones (LJ) fluid, a model system which captures all basic physical aspects of non-polar fluids, the MBWR equation has been one of the most successful up to now, even more successful than many available 'semi-theoretical' equations of state, i.e. the ones which are partly based on statistical mechanics [4].

However, the MBWR equation, like other empirical equations of state, is accurate only within a limited temperature range: after the parametrizations by Nicolas *et al.* [5] and Johnson *et al.* [4] for the (reduced) temperature range $0.75 \leqslant T \leqslant 6.0$, largely based on molecular dynamics and Monte Carlo simulation data, new parameters were obtained to improve the 'low temperature' ($0.45 \leqslant T \leqslant 0.85$) range by Sun and Teja [6].

All empirical equations of state lack (by definition) a firm foundation in the statistical mechanics of fluids. In general, they can only be used as a local description

*Author for correspondence. e-mail: amadei@monet.chem.uniroma1.it

Downloaded By: [EBSCOHost EJS Content Distribution] At: 14:09 25 March 2008

within the range in which the parameters were obtained, and often they have difficulties reproducing properly temperature and density derivatives of the free energy, such as the heat capacity.

The semi-theoretical EOS, often based on simple perturbation expansions, are accurate if a pure empirical part is added. This implies that also for these equations, temperature and density extrapolations outside the parametrization range may not be accurate, and often properties which were not used in the parametrization are not reliable even within the parametrization range. The most recent semi-theoretical EOS for LJ fluids are the Kolafa–Nezbeda (KN) [7] and Mecke *et al.* (VDW) [8] ones. The KN equation is based on a first order perturbation expansion with respect to a temperature dependent hard-sphere reference, combined with an empirical temperature-density polynomial. In the Mecke *et al.* VDW equation the hard-sphere reference is directly combined with an empirical polynomial. In both equations the temperature dependence of the hard-sphere reference is obtained by the hybrid Barker–Henderson theory [9] which links the LJ potential with the hard-sphere diameter at every temperature. In their parametrization ranges these EOS can be more accurate than the MBWR equations but still could have the problems previously mentioned, due to the presence of pure empirical terms for the temperature and density dependence.

In this paper we will present a new equation of state, based on the quasi-Gaussian entropy (QGE) theory. This is a statistical mechanical approach based on probability distribution functions of fluctuations inside the system, instead of the usual partition functions. In recent articles we illustrated its basic form for the three main statistical ensembles: the canonical ensemble (NVT) using the energy [10] or excess energy [11] fluctuations, the isothermal–isobaric ensemble (NpT) using the enthalpy [10] or volume [12] fluctuations, and the grand canonical ensemble (μVT) using the grand canonical heat function [10] or fluctuations of the number of particles [12]. For each of these three ensembles we applied the theory at the level of Gamma or Gamma-like (e.g. Inverse Gaussian) probability distributions, which are the types of physically allowed distributions just beyond the simplest one, the Gaussian. Application to different kinds of molecules showed that Gamma distributions can be used successfully to describe the thermodynamics of fluids. Hence the corresponding Gamma 'statistical state' can be considered as a general theoretical model for fluid systems.

In particular, in the canonical ensemble the Gamma statistical state based on the excess energy provided an excellent description of the thermodynamics along isochores over a large range of density and temperature, and was applicable to virtually all the usual fluid phase conditions [11, 13, 14].

These results strongly suggest that the Gamma statistical state can be an excellent model to obtain a general EOS, really based on a coherent physical theory. In this paper we use the previously introduced confined Gamma statistical state [11] for the excess energy fluctuations (NVT ensemble), in combination with a simple perturbation term, which will be derived in section 2.2. Assuming the resulting perturbed confined Gamma state to be virtually an exact statistical state at every density, at least within the density range of interest, we can build up in a simple way a complete equation of state. In fact, the temperature dependence along each isochore is directly provided by the perturbed confined Gamma state, if the parameters of the excess free energy expression and those of the pressure expression are known at the arbitrary reference isotherm T_0. Such parameters correspond to different physical properties of the system at the reference isotherm, depending only on the density.

In this article we obtain them from molecular dynamics simulation data, and two approaches will be used to obtain an EOS. Firstly, we will evaluate from energy and pressure data the necessary free energy and pressure input properties at T_0 for a set of densities, and hence the temperature along the corresponding isochores will be obtained (discrete density equation of state, DD EOS). Secondly, we will obtain the density dependence of the free energy input properties, by interpolating a set of thermodynamic properties related to these at the reference isotherm T_0 by simple polynomials. In this way we obtain a fully analytical equation (continuous density equation of state, CD EOS).

The resulting equations of state will be applied to the LJ fluid in the density range 0–1.0 (in reduced units), using for both DD and CD equations two temperature ranges for their parametrization: a large temperature range ($1.0 \leqslant T \leqslant 20.0$) and a smaller one ($1.0 \leqslant T \leqslant 6.0$). For the parametrization of both CD EOS only energy data were used except at the reference isotherm $T_0 = 2.0$, where also pressure data were involved. Conversely, the DD EOS parametrizations involved for each isochore both energy and pressure data. The two parametrizations for the DD and CD equations provide an excellent description of the thermodynamics in a very large temperature–density range, and also are able to reproduce with high accuracy properties which were not involved in the parametrization, like the heat capacity or, for the CD EOS, the pressure. Remarkably, the parametrization in the smaller temperature range ($1.0 \leqslant T \leqslant 6.0$) gives results which are extremely close to the ones obtained from the large temperature range ($1.0 \leqslant T \leqslant 20.0$), even at the highest temperatures.

Downloaded By: [EBSCOHost EJS Content Distribution] At: 14:09 25 March 2008

The article is organized as follows. In section 2 we describe the temperature dependence of the EOS, giving a summary of the QGE theory [11, 14] (section 2.1) and introducing the perturbation (section 2.2). In section 3 we describe in general how to obtain the input properties of the perturbed Gamma state and the models used for the interpolation. In sections 4 and 5 we give technical details on the molecular dynamics simulations and parametrization procedure. Finally, in sections 6 and 7 we discuss the results obtained, also comparing our EOS with the MBWR, KN and VDW equations and give some general conclusions.

2. Temperature dependence

For the temperature dependence along isochores we will use a perturbed confined Gamma state, based on the confined Gamma state previously introduced [11, 14] which will be reviewed in section 2.1. The perturbation will be described in section 2.2.

2.1. *Basic theory and confined Gamma state*

The Helmholtz free energy in the canonical ensemble is given by

$$A = -kT \ln Q, \tag{1}$$

$$Q \cong \frac{1}{N!} Q^{\mathrm{e}} Q^{\mathrm{kin}} Q^{\mathrm{pot}}, \tag{2}$$

where N is the number of molecules, Q^{e} is the electronic partition function, Q^{kin} is the kinetic energy partition function, defined by the momenta of the system, including the Planck constants. Q^{pot} is the configurational partition function, which can be expressed, using the general approximation previously introduced [11], as

$$Q^{\mathrm{pot}} \cong Q^{v}_{\mathrm{id}} \int^{\prime *} \exp(-\beta \mathcal{U}') \, \mathrm{d}\mathbf{x}, \tag{3}$$

with

$$\mathcal{U}' = \Phi + \psi + \mathcal{E}^0 - E^0_{\mathrm{id}} \tag{4}$$

the ideal reduced (or 'potential') energy. In these expressions $\mathbf{x}$ are the atomic coordinates, Φ is the intermolecular potential energy and ψ the intramolecular potential energy (excluding bond length and bond angle vibrational energies). E^0_{id} and Q^{v}_{id} are the overall vibrational ground state energy and vibrational partition function of the ideal gas ($\Phi = 0$), $\mathcal{E}^0$ is the overall vibrational ground state energy of the actual system and $\beta = 1/kT$. The prime on the integral means that we integrate only over configurations where all the bond lengths and angles are fixed. The star denotes an integration over the accessible part of the configurational space only [11], assuming that a (temperature independent) part of the configurational space of the corresponding ideal gas is inaccessible for the actual system due to 'excluded volume' effects.

We define the *ideal* reference state as

$$A_{ref} = -kT \ln Q_{\mathrm{ref}}, \tag{5}$$

$$Q_{\mathrm{ref}} = \frac{1}{N!} Q^{\mathrm{e}} Q^{\mathrm{kin}} Q^{\mathrm{pot}}_{\mathrm{ref}}, \tag{6}$$

$$Q^{\mathrm{pot}}_{\mathrm{ref}} = Q^{v}_{\mathrm{id}} \int^{\prime} \mathrm{d}\mathbf{x}, \tag{7}$$

and the *confined ideal* reference state as

$$A_{*\mathrm{ref}} = -kT \ln Q_{*ref}, \tag{8}$$

$$Q_{*\mathrm{ref}} = \frac{1}{N!} Q^{\mathrm{e}} Q^{\mathrm{kin}} Q^{\mathrm{pot}}_{*\mathrm{ref}}, \tag{9}$$

$$Q^{\mathrm{pot}}_{*\mathrm{ref}} = Q^{v}_{\mathrm{id}} \int^{\prime *} \mathrm{d}\mathbf{x}. \tag{10}$$

The difference between the two states is merely the integration limits in configurational space: the full configurational volume of the ideal gas in equation (7), and the configurational volume of the actual system with possible excluded volume effects in equation (10). We can express the ideal reduced (A') and confined ideal reduced (A^*) free energies as excess properties in the following way:

$$A' = A - A_{\mathrm{ref}} = A^* - kT \ln \varepsilon, \tag{11}$$

$$A^* = A - A_{*\mathrm{ref}} = kT \ln G_{\mathcal{U}'}(\beta), \tag{12}$$

where

$$G_{\mathcal{U}'}(\beta) = \langle \exp(\beta \mathcal{U}') \rangle = \int \exp(\beta \mathcal{U}') \rho(\mathcal{U}') \, \mathrm{d}\mathcal{U}' = \frac{Q^{\mathrm{pot}}_{*\mathrm{ref}}}{Q^{\mathrm{pot}}} \tag{13}$$

is the moment generating function (MGF) [15–17] of the energy probability distribution function $\rho(\mathcal{U}')$, and

$$\varepsilon = \frac{\int^{\prime *} \mathrm{d}\mathbf{x}}{\int^{\prime} \mathrm{d}\mathbf{x}} \tag{14}$$

is the fraction of configurational space which is accessible to the system. The ideal reduced and confined ideal reduced internal energy, heat capacity, entropy and pressure are given by

Downloaded By: [EBSCOHost EJS Content Distribution] At: 14:09 25 March 2008

$$U' = -\left(\frac{\partial}{\partial\beta}\ln\frac{Q^{\text{pot}}}{Q^{\text{pot}}_{\text{ref}}}\right)_V = \langle \mathcal{U}'\rangle = U^*, \tag{15}$$

$$C'_V = \left(\frac{\partial U'}{\partial T}\right)_V = C^*_V, \tag{16}$$

$$S' = -\frac{(A' - U')}{T} = S^* + k\ln\varepsilon, \tag{17}$$

$$S^* = -k\ln G_{\mathcal{U}'}(\beta) + U^*/T, \tag{18}$$

$$p' = -\left(\frac{\partial A'}{\partial V}\right)_T = p^* + T\xi, \tag{19}$$

$$p^* = -\left(\frac{\partial A^*}{\partial V}\right)_T, \tag{20}$$

where

$$\xi = k\frac{\mathrm{d}\ln\varepsilon}{\mathrm{d}V}. \tag{21}$$

Due to the central limit theorem [15, 17], in a macroscopic system the energy distribution must be close to a Gaussian, and hence it is possible to model the energy probability density $\rho(\mathcal{U}')$ and its moment generating function $G_{\mathcal{U}'}(\beta) = \langle\exp(\beta\mathcal{U}')\rangle = \int\exp(\beta\mathcal{U}')\rho(\mathcal{U}')\,\mathrm{d}\mathcal{U}'$ via a generalized Pearson system for unimodal curves [11, 18]. The parameters of the probability distribution, which in general depend on temperature, can be expressed in terms of the central energy moments $M_n = \langle(\mathcal{U}' - U^*)^n\rangle$ and these in turn via statistical mechanics in terms of C^*_V and its temperature derivatives. We thus obtain a closed ordinary differential equation, the thermodynamic master equation (TME) [11, 18], the solutions of which provide the whole thermodynamics along an isochore. The distribution completely determines the thermodynamics, and so the *statistical state* of the system. We showed that the use of a Gamma distribution (giving rise to a Gamma statistical state) to model $\rho(\mathcal{U}')$ and $G_{\mathcal{U}'}(\beta)$ reproduces very well the thermodynamics of different types of molecules, both polar (water) and non-polar (methane), over a large temperature-density range. Hence this statistical state can be considered as a general condition for fluids. For the Gamma state, with energy distribution

$$\rho(\mathcal{U}') = \frac{\theta^a}{\Gamma(a)}(\mathcal{U}' - \mathcal{U}'_m)^{a-1}\exp\{-\theta(\mathcal{U}' - \mathcal{U}'_m)\}, \tag{22}$$

where the parameters a, θ and $\mathcal{U}'_m$ can be expressed in terms of U^*, C^*_V and $\partial C^*_V/\partial T$, the confined ideal reduced properties are [11]

$$C^*_V(T) = C^*_{V0}\left(\frac{\delta(T)}{\delta_0}\right)^2, \tag{23}$$

$$S^*(T) = \frac{C^*_{V0}}{\delta_0^2}\left[\delta(T) + \ln\{1 - \delta(T)\}\right], \tag{24}$$

$$U^*(T) = U^*_0 + (T - T_0)\,C^*_{V0}\,\frac{\delta(T)}{\delta_0}, \tag{25}$$

$$A^*(T) = U^*_0 - \frac{T_0 C^*_{V0}}{\delta_0} - \frac{T C^*_{V0}}{\delta_0^2}\ln\{1 - \delta(T)\}, \tag{26}$$

$$p^*(T) = p^*_0 + B^*_0 + B^*_1\frac{T}{T(1-\delta_0) + T_0\delta_0} + B^*_2\left(\frac{T}{T_0}\right)\ln\left\{\frac{T(1-\delta_0)}{T(1-\delta_0) + T_0\delta_0}\right\}, \tag{27}$$

where δ follows from the TME

$$\delta(T) = \frac{T_0\delta_0}{T(1-\delta_0) + T_0\delta_0}, \tag{28}$$

$$\delta_0 = \frac{T_0(\partial C^*_{V0}/\partial T)_V}{2C^*_{V0}} + 1 \tag{29}$$

and

$$B^*_i = A_{i1}T_0\left(\frac{\partial p^*_0}{\partial T}\right)_V + A_{i2}T_0^2\left(\frac{\partial^2 p^*_0}{\partial T^2}\right)_V, \quad i = 0, 1, 2, \tag{30}$$

with

$$A_{01} = -\frac{2(1-\delta_0)\ln(1-\delta_0) + \delta_0}{D},$$

$$A_{02} = \frac{1}{\delta_0}\frac{(1-\delta_0)\ln(1-\delta_0) + \delta_0}{D},$$

$$A_{11} = \frac{\delta_0}{D},$$

$$A_{12} = -\frac{1}{\delta_0}\frac{\ln(1-\delta_0) + \delta_0}{D},$$

$$A_{21} = \frac{2(1-\delta_0)}{D},$$

$$A_{22} = \frac{1}{D}, \tag{31}$$

and

$$D = 2(1-\delta_0)\ln(1-\delta_0) + \delta_0(2-\delta_0). \tag{32}$$

A zero subscript denotes properties evaluated at the arbitrary reference temperature T_0. Note that equations (23)–(26), combined with equations (15)–(17), express the free energy and all its temperature derivatives along an isochore from the knowledge of four input properties at T_0: U^*, C^*_V, $\partial C^*_V/\partial T$ and ε. In addition, the pressure and its temperature derivatives follow from

Downloaded By: [EBSCOHost EJS Content Distribution] At: 14:09 25 March 2008

equation (7), combined with equation (19), using four additional input parameters at T_0: p^*, $\partial p^*/\partial T$, $\partial^2 p^*/\partial T^2$ and ξ.

2.2. *The perturbed confined Gamma state*

The fact that the fluid thermodynamics can be described by Gamma states with high accuracy over a large range of temperature and density, implies that the exact statistical states of fluid systems must be some kind of perturbed Gamma state, where such a perturbation is in general small and often negligible. We can explicitly introduce the perturbation by considering that for a system in a perturbed Gamma state it is possible to decompose the configurational integrals in equations (3) and (10) as

$$\int'^{*} \exp(-\beta\mathcal{U}')\,\mathrm{d}\mathbf{x} = \int'^{\Gamma} \exp(-\beta\mathcal{U}')\,\mathrm{d}\mathbf{x} + \int'^{P} \exp(-\beta\mathcal{U}')\,\mathrm{d}\mathbf{x} \quad (33)$$

and

$$\int'^{*} \mathrm{d}\mathbf{x} = \int'^{\Gamma} \mathrm{d}\mathbf{x} + \int'^{P} \mathrm{d}\mathbf{x}, \quad (34)$$

where the Γ superscript means that the integrals are over the part of accessible configurational space which can be exactly described by a Gamma state over the whole temperature range and P denotes integration over the remaining perturbation part of the accessible configurational space, see also figure 1.

Using equations (33) and (34) we can rewrite equation (11) as

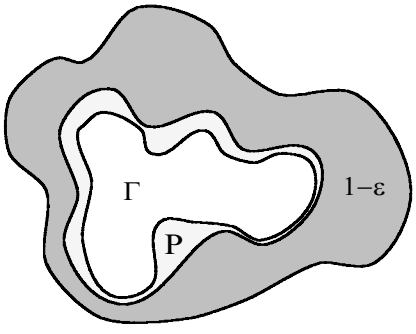

Figure 1. Schematic view of configurational space and the different regions of equations (33) and (34): dark grey denotes the inaccessible part (with fraction $1-\varepsilon$), the inner part (with fraction ε) is accessible and divided into a Gamma region (Γ) and a small perturbation region (P).

$$A' = -kT \ln\left(\frac{\int'^{*} \exp(-\beta\mathcal{U}')\,\mathrm{d}\mathbf{x}}{\int'^{\Gamma} \exp(-\beta\mathcal{U}')\,\mathrm{d}\mathbf{x}}\right) - kT \ln\left(\frac{\int'^{\Gamma} \exp(-\beta\mathcal{U}')\,\mathrm{d}\mathbf{x}}{\int'^{\Gamma} \mathrm{d}\mathbf{x}}\right) - kT \ln\left(\frac{\int'^{\Gamma} \mathrm{d}\mathbf{x}}{\int'^{*} \mathrm{d}\mathbf{x}}\right) - kT \ln \varepsilon, \quad (35)$$

where

$$-kT \ln\left(\frac{\int'^{\Gamma} \exp(-\beta\mathcal{U}')\,\mathrm{d}\mathbf{x}}{\int'^{\Gamma} \mathrm{d}\mathbf{x}}\right) \equiv A^*_\Gamma \quad (36)$$

is the Helmholtz free energy of the Gamma region, which is given by equation (26). In fact, equation (36) implies that there exists a TME for the Gamma part of configurational space only, with as solution the properties given by equations (23)–(27). In the last term of equation (35), ε is as usual the fraction of accessible configurational space with respect to the whole (ideal gas) one, equation (14), and $(\int'^{\Gamma} \mathrm{d}\mathbf{x}/\int'^{*} \mathrm{d}\mathbf{x})$ in the third term is the fraction of the Gamma part within the accessible part of configurational space, see also figure 1. If we use a Padé approximant [19, 20] in β for the first term in equation (35), the perturbation, we have

$$-k \ln\left(\frac{\int'^{*} \exp(-\beta\mathcal{U}')\,\mathrm{d}\mathbf{x}}{\int'^{\Gamma} \exp(-\beta\mathcal{U}')\,\mathrm{d}\mathbf{x}}\right) \cong \frac{F_1^m(\beta)}{F_2^n(\beta)}, \quad (37)$$

where $F_1^m(\beta)$ and $F_2^n(\beta)$ are two polynomials in β of order m and n. Hence

$$A' = A^*_\Gamma + T\frac{F_1^m(\beta)}{F_2^n(\beta)} - kT \ln\left(\frac{\int'^{\Gamma} \mathrm{d}\mathbf{x}}{\int'^{*} \mathrm{d}\mathbf{x}}\right) - kT \ln \varepsilon. \quad (38)$$

In the case $m = n = 0$, i.e. a $[0/0]$ approximant [12], the perturbation term becomes a constant in β and the perturbed Gamma state is completely equivalent to a pure confined Gamma state. The expansion of immediate higher complexity is either a $[1/0]$ or $[0/1]$ approximant. While in the former case we obtain again a confined Gamma state with a constant shift for the internal energy, in the latter case we obtain a perturbed

Downloaded By: [EBSCOHost EJS Content Distribution] At: 14:09 25 March 2008

Gamma state that really goes beyond a usual confined Gamma state. The perturbation term is in this case simply

$$-k \ln \left(\frac{\int'^{*} \exp(-\beta \mathcal{U}') \, d\mathbf{x}}{\int'^{\Gamma} \exp(-\beta \mathcal{U}') \, d\mathbf{x}} \right) \cong \frac{a_0}{b_0 + b_1 \beta} = \frac{\lambda T}{T + \gamma}, \quad (39)$$

where $\lambda = a_0/b_0$ and $\gamma = b_1/kb_0$. Considering that from equation (39)

$$\lim_{T \to \infty} -k \ln \left(\frac{\int'^{*} \exp(-\beta \mathcal{U}') \, d\mathbf{x}}{\int'^{\Gamma} \exp(-\beta \mathcal{U}') \, d\mathbf{x}} \right) = +k \ln \left(\frac{\int'^{\Gamma} d\mathbf{x}}{\int'^{*} d\mathbf{x}} \right) \cong \lambda \quad (40)$$

we can rewrite equation (38) as

$$A' = A'^{*}_{\Gamma} + \frac{\lambda T^2}{T + \gamma} - \lambda T - kT \ln \varepsilon = A'^{*}_{\Gamma} - \frac{\lambda \gamma T}{T + \gamma} - kT \ln \varepsilon. \quad (41)$$

So the physical meaning of λ is related to the fraction of the accessible configurational space that is associated with the Gamma state, and hence λ must be always zero or negative.

Moreover, since

$$-\frac{\partial}{\partial \beta} \ln \left(\frac{\int'^{*} \exp(-\beta \mathcal{U}') \, d\mathbf{x}}{\int'^{\Gamma} \exp(-\beta \mathcal{U}') \, d\mathbf{x}} \right) = U^* - U^*_{\Gamma} \cong -\frac{\lambda \gamma T^2}{(T + \gamma)^2}, \quad (42)$$

where U^*_{Γ} is the ideal reduced internal energy corresponding to the Gamma part of configurational space, given by equation (25), we find for the infinite temperature limit

$$\lim_{T \to \infty} U^* - U^*_{\Gamma} \equiv \Delta U_{\max} \cong -\lambda \gamma, \quad (43)$$

where $\Delta U_{\max}$ is the difference in the ideal reduced internal energy corresponding to the whole accessible phase space and the one corresponding to the Gamma part only, at infinite temperature. This gives a physical interpretation to γ as well. Note that the infinite temperature limit of the ideal reduced internal energy is a finite value (see [11] and [14]), and that from this last equation follows that γ and $\Delta U_{\max}$ must always have the same sign.

For the low temperature limit of $U^* - U^*_{\Gamma}$ we should distinguish two different cases.

If $\gamma > 0$, the perturbation term is defined down to $T = 0$ and from equation (42) we have

$$\lim_{T \to 0} U^* - U^*_{\Gamma} \cong 0, \quad (44)$$

which implies that the ground state energy of the system lies within the Gamma part of accessible configurational space. The perturbation therefore deals for the greater part with high energy configurations, i.e. the right-hand tail of the energy distribution $\rho(\mathcal{U}')$.

If $\gamma < 0$, there is a singularity at temperature $T_s = -\gamma$, where the perturbation term becomes infinite. Hence

$$\lim_{T \to T_s} U^* - U^*_{\Gamma} \cong -\infty. \quad (45)$$

Such a condition should be considered as an approximation in the case where the ground state energy does not belong to the Gamma part of phase space, and the perturbation deals with the low-energy configurations, i.e. the left-hand tail of $\rho(\mathcal{U}')$. In fact, a real mathematical singularity can only occur at $T = 0$. So for densities where the perturbed Gamma state is virtually the exact state, T_s must be regarded as a limit temperature which defines the interval $[0, T_s]$, where the perturbation term is numerically diverging.

Hence for this simplest perturbed confined Gamma state we finally obtain

$$A' = A'^{*}_{\Gamma} + \frac{\Delta U_{\max} T}{T + \gamma} - kT \ln \varepsilon, \quad (46)$$

$$U' = U'^{*}_{\Gamma} + \frac{\Delta U_{\max} T^2}{(T + \gamma)^2}, \quad (47)$$

$$S' = S'^{*}_{\Gamma} - \frac{\Delta U_{\max} \gamma}{(T + \gamma)^2} + k \ln \varepsilon, \quad (48)$$

$$C'_V = C'^{*}_{V\Gamma} + 2 \frac{\Delta U_{\max} \gamma T}{(T + \gamma)^3}, \quad (49)$$

$$p' = p'^{*}_{\Gamma} + \xi T - \left(\frac{d \Delta U_{\max}}{dV} \right) \frac{T}{T + \gamma} + \left(\frac{d\gamma}{dV} \right) \frac{\Delta U_{\max} T}{(T + \gamma)^2}, \quad (50)$$

where clearly A'^{*}_{Γ}, U'^{*}_{Γ}, S'^{*}_{Γ}, $C'^{*}_{V\Gamma}$ and p'^{*}_{Γ} are given by equations (23)–(27), and if $\Delta U_{\max} = \gamma = 0$, equations (46)–(50) reduce to the confined Gamma state expressions. With respect to the confined Gamma state equations we have introduced two additional parameters, $\Delta U_{\max}$ and γ, and their volume derivatives to obtain the full thermodynamics along an isochore. *In the remainder of*

Downloaded By: [EBSCOHost EJS Content Distribution] At: 14:09 25 March 2008

this article, we will denote by a Γ subscript the properties that correspond to the Gamma part of configurational space.

3. Density dependence

To build a complete equation of state we assume that the perturbed confined Gamma state, given by equations (46)–(50), is the correct statistical state at every density, at least inside the density range of interest. A strong theoretical advantage to choosing the isochore description as a general one is the fact that it is based on fluctuations of the 'potential' energy $\mathcal{U}'$, which are in general well converging even close to the critical point, although at the critical point, according to the critical point fluctuation theory, these fluctuations and hence C_V^* should diverge [21]. This is in contrast with the volume fluctuations, which are clearly infinite at the critical point but also tend to diverge in the critical point region. We therefore do not expect that the critical point and coexistence region will create severe difficulties for this equation of state, based on the isochore perturbed Gamma state for the potential energy. Moreover, if we would assume that the *isotherm* description using the Gamma level of the QGE theory for density fluctuations (e.g. the diverging Gamma state for the volume [12]) is the general statistical state at every temperature, the resulting EOS does not allow phase separations in the system, since the pressure along each isotherm is in that case monotonically increasing with density. Conversely, with the present choice that the Gamma level *isochore* description is the general statistical state, it is always possible to obtain an EOS which allows phase separations.

Equations (46)–(50) provide directly the equation of state if we have the explicit density dependence of the properties $U_{\Gamma 0}^*$, $C_{V\Gamma 0}^*$, δ_0, $\Delta U_{\max}$, γ and ε, or of any other six independent thermodynamic properties at the reference isotherm T_0. Note that for the pressure equation (equation (50) with (27) and (30)), besides $\mathrm{d}\Delta U_{\max}/\mathrm{d}V$, $\mathrm{d}\gamma/\mathrm{d}V$ and $\xi = k\,\mathrm{d}\ln\varepsilon/\mathrm{d}V$, also $p_{\Gamma 0}^*$, $(\partial p_{\Gamma 0}^*/\partial T)_V$ and $(\partial^2 p_{\Gamma 0}^*/\partial T^2)_V$ can be obtained via thermodynamic relations in terms of volume derivatives of $U_{\Gamma 0}^*$, $C_{V\Gamma 0}^*$ and δ_0. Also note that the Γ subscripts refer to the properties in equations (23)–(27) which describe the Gamma part of configurational space only.

We can directly obtain the input properties needed (excluding ε), relating them to proper physical 'observables' at the reference isotherm T_0, the energy (equation (47)) and its temperature derivatives:

$$U_0^* = U_{\Gamma 0}^* + \Delta U_{\max}\,\frac{T_0^2}{(T_0+\gamma)^2}, \tag{51}$$

$$T_0 C_{V0}^* = T_0 C_{V\Gamma 0}^* + 2\Delta U_{\max}\,\frac{T_0^2\gamma}{(T_0+\gamma)^3}, \tag{52}$$

$$T_0^2\frac{\partial C_{V0}^*}{\partial T} = -2T_0 C_{V\Gamma 0}^*(1-\delta_0) - 2\Delta U_{\max}\,\frac{T_0^2\gamma(2T_0-\gamma)}{(T_0+\gamma)^4}, \tag{53}$$

$$T_0^3\frac{\partial^2 C_{V0}^*}{\partial T^2} = 6T_0 C_{V\Gamma 0}^*(1-\delta_0)^2 + 12\Delta U_{\max}\,\frac{T_0^3\gamma(T_0-\gamma)}{(T_0+\gamma)^5}, \tag{54}$$

$$T_0^4\frac{\partial^3 C_{V0}^*}{\partial T^3} = -24T_0 C_{V\Gamma 0}^*(1-\delta_0)^3 - 24\Delta U_{\max}\,\frac{T_0^4\gamma(2T_0-3\gamma)}{(T_0+\gamma)^6}, \tag{55}$$

where equations (51)–(55) can be used as a system to express our input properties if the energy and its temperature derivatives are known along the reference isotherm. In the case a model for the molecular potential is available, as for the LJ fluid, we could in principle calculate explicitly the central moments of the potential energy and hence obtain the energy and its temperature derivatives for equations (51)–(55) from the statistical mechanical relations [14]

$$U_0^* = \langle \mathcal{U}' \rangle_0, \tag{56}$$

$$T_0 C_{V0}^* = \left(\frac{1}{kT_0}\right)^2 [M_{2,0}], \tag{57}$$

$$T_0^2\frac{\partial C_{V0}^*}{\partial T} = \left(\frac{1}{kT_0}\right)^2 [M_{3,0} - 2kT_0 M_{2,0}], \tag{58}$$

$$T_0^3\frac{\partial^2 C_{V0}^*}{\partial T^2} = \left(\frac{1}{kT_0}\right)^3 [M_{4,0} - 6kT_0 M_{3,0} + 6(kT_0)^2 M_{2,0} - 3M_{2,0}^2], \tag{59}$$

$$T_0^4\frac{\partial^3 C_{V0}^*}{\partial T^3} = \left(\frac{1}{kT_0}\right)^4 [M_{5,0} - 12kT_0 M_{4,0} + 36(kT_0)^2 M_{3,0} - 10M_{3,0}M_{2,0} + 36kT_0 M_{2,0}^2 - 24(kT_0)^3 M_{2,0}], \tag{60}$$

where $M_{n,0} = \langle (\mathcal{U}' - U_0^*)^n \rangle_0$ is the nth central potential energy moment for a given density at the reference isotherm. Similarly, differentiating equations (51)–(55) in the volume and using thermodynamic relations which link heat capacity volume derivatives to temperature derivatives of the pressure, we can obtain a new system of equations for the input derivatives needed for the pressure expression. Again, from the molecular potential we could in principle obtain these pressure derivatives along the reference isotherm directly calcu-

Downloaded By: [EBSCOHost EJS Content Distribution] At: 14:09 25 March 2008

lating correlation terms between the instantaneous energy and virial with equations analogous to equations (56)–(60). Finally, we could estimate also the 6th parameter, the confinement term $k \ln \varepsilon$ and its volume derivative ξ by comparing at every density A_0^* and p_0^*, obtained from our theory, with p_0' and A_0' (which can be calculated by numerically integrating p_0' in the density), obtained either from experiment or from direct calculation of the virial with a model potential.

In this way the full equation of state could be defined from the knowledge of only a limited set of physical properties at the reference isotherm. Unfortunately, such a direct way cannot be used, as for any arbitrary reference isotherm chosen, the required high order temperature derivatives of the heat capacity and pressure are beyond the available accuracy. Even in the case of the LJ fluid, where a model potential is present, the direct calculations of high order central moments of energy and virial-energy correlations are beyond present computational power.

Hence we were forced to follow a different strategy, using for each isochore energy values obtained, at least, at five different temperatures in order to evaluate the input properties. Similarly using pressure values at least at five different temperatures at each isochore, it is possible to obtain also the pressure input properties. So if the confinement fraction and its volume derivative are known (see above), the full discrete density (DD) equation of state can be obtained. For densities in between subsequent isochores where the input properties were evaluated, a local numerical interpolation can be used.

In order to simplify the EOS and severely test the intrinsic coherence of the simulations and the power of the theory, we will also use a different approach (continuous density (CD) equation). From the free energy input parameters obtained for a set of densities and pressure values only at the reference isotherm, we calculate six independent thermodynamic properties per isochore along the reference isotherm. Afterwards these six properties were interpolated in the whole density range of interest by fitting their values with simple model functions.

We chose as independent properties A_0^*, U_0^*, C_{V0}^*, $S_{\Gamma 0}^*$, $C_{V\Gamma 0}^*$ and ε, as they are basic thermodynamic quantities for which we do not expect a too complex density behaviour.

From these last properties we can retrieve the density dependence of the 'natural parameters' of the equation of state, $U_{\Gamma 0}^*$, δ_0, $\Delta U_{\max}$ and γ, by inversion of equations (46)–(70):

$$\gamma = -T_0\left[1 + 2\left(\frac{S_0^* - S_{\Gamma 0}^*}{C_{V0}^* - C_{V\Gamma 0}^*}\right)\right], \tag{61}$$

$$\Delta U_{\max} = \frac{(C_{V0}^* - C_{V\Gamma 0}^*)(T_0 + \gamma)^3}{2T_0\gamma}, \tag{62}$$

$$U_{\Gamma 0}^* = A_0^* + T_0 S_{\Gamma 0}^* - \frac{\Delta U_{\max} T_0}{T_0 + \gamma}, \tag{63}$$

where clearly $S_0^* = S_0' - k \ln \varepsilon = (U_0^* - A_0^*)/T_0$. Furthermore, δ_0 can be solved numerically from

$$\frac{S_{\Gamma 0}^*}{C_{V\Gamma 0}^*} = \frac{1}{\delta_0} + \frac{1}{\delta_0^2}\ln(1 - \delta_0). \tag{64}$$

From the pressure equation (equation (50)) and its first and second temperature derivatives, we obtain the required input derivatives for the pressure expressions (equations (50), (27) and (30)) (see equations (65–67)); where we have defined for convenience

$$L_1 = -\frac{T_0}{T_0 + \gamma},$$

$$L_2 = \frac{\Delta U_{\max} T_0}{(T_0 + \gamma)^2},$$

$$W_1 = -\frac{\gamma}{(T_0 + \gamma)^2},$$

$$W_2 = -\frac{\Delta U_{\max}}{(T_0 + \gamma)^2}\left(1 - \frac{2\gamma}{T_0 + \gamma}\right),$$

$$\frac{\mathrm{d}\gamma}{\mathrm{d}V} = \frac{W_1\left[\left(\frac{\partial^2 p_0^*}{\partial T^2}\right)_V - \left(\frac{\partial^2 p_{\Gamma 0}^*}{\partial T^2}\right)_V\right] - Z_1\left[\left(\frac{\partial p_0^*}{\partial T}\right)_V - \left(\frac{\partial p_{\Gamma 0}^*}{\partial T}\right)_V\right]}{W_1 Z_2 - W_2 Z_1}, \tag{65}$$

$$\frac{\mathrm{d}\Delta U_{\max}}{\mathrm{d}V} = -\frac{W_2\left[\left(\frac{\partial^2 p_0^*}{\partial T^2}\right)_V - \left(\frac{\partial^2 p_{\Gamma 0}^*}{\partial T^2}\right)_V\right] - Z_2\left[\left(\frac{\partial p_0^*}{\partial T}\right)_V - \left(\frac{\partial p_{\Gamma 0}^*}{\partial T}\right)_V\right]}{W_1 Z_2 - W_2 Z_1} \tag{66}$$

$$p_{\Gamma 0}^* = p_0^* - L_1\frac{\mathrm{d}\Delta U_{\max}}{\mathrm{d}V} - L_2\frac{\mathrm{d}\gamma}{\mathrm{d}V}, \tag{67}$$

Downloaded By: [EBSCOHost EJS Content Distribution] At: 14:09 25 March 2008

$$Z_1 = \frac{2\gamma}{(T_0+\gamma)^3},$$

$$Z_2 = \frac{2\Delta U_{\max}}{(T_0+\gamma)^3}\left(1-\frac{3\gamma}{T_0+\gamma}\right), \tag{68}$$

The temperature derivatives of the pressures p^* and p^*_Γ, appearing in equations (65) and (66), can be easily expressed via Maxwell relations as volume derivatives of S^*, S^*_Γ, C^*_V and $C^*_{V\Gamma}$, which are modelled via simple analytical polynomials as a function of volume:

$$\left(\frac{\partial p^*_0}{\partial T}\right)_V = \left(\frac{\partial S^*_0}{\partial V}\right)_T,$$

$$\left(\frac{\partial p^*_{\Gamma 0}}{\partial T}\right)_V = \left(\frac{\partial S^*_{\Gamma 0}}{\partial V}\right)_T,$$

$$T_0\left(\frac{\partial^2 p^*_0}{\partial T^2}\right)_V = \left(\frac{\partial C^*_{V0}}{\partial V}\right)_T,$$

$$T_0\left(\frac{\partial^2 p^*_{\Gamma 0}}{\partial T^2}\right)_V = \left(\frac{\partial C^*_{V\Gamma 0}}{\partial V}\right)_T. \tag{69}$$

For the confinement fraction ε we used in both DD and CD equations the simple hard-sphere model based on the Carnahan–Starling equation of state [22], which proved to be an excellent description of the phase-space confinement of small molecules like water [11]:

$$k\ln\varepsilon = Nk\frac{(3\eta^2-4\eta)}{(1-\eta)^2}, \tag{70}$$

$$\xi = k\frac{\mathrm{d}\ln\varepsilon}{\mathrm{d}V} = -\rho_N k\frac{(2\eta^2-4\eta)}{(1-\eta)^3}, \tag{71}$$

with

$$\eta = \rho_N v \tag{72}$$

the packing fraction, where $\rho_N = N/V$ is the molecular density, $v = \pi\sigma^3_{\mathrm{HS}}/6$ the hard sphere volume per molecule and σ_{HS} the corresponding hard sphere diameter. This clearly reduces ε and ξ to one parameter, i.e. v.

For the CD equations we treated the density dependence of the other parameters by simple interpolating functions. To obtain the density dependence of A^*_0 (and A'_0), the pressure at T_0 was modelled using a $[10/1]$ Padé approximant. This, via expansion, is a generalization of the $[0/1]$ expression, which corresponds to a diverging Gamma state for the volume fluctuations [12]

$$p_0 = \frac{kT_0\rho_N + a'_0\rho_N^2 + \cdots + a'_8\rho_N^{10}}{1-a'_9\rho_N}$$

$$= a_0\rho_N + a_1\rho_N^2 + \cdots + a_8\rho_N^9 + \frac{(kT_0-a_0)\rho_N}{1-a_9\rho_N} \tag{73}$$

after reorganizing the terms. The ideal reduced and confined ideal reduced pressures are now given by

$$p'_0 = p_0 - \rho_N kT_0, \tag{74}$$

$$p^*_0 = p_0 - (\xi+\rho_N k)T_0. \tag{75}$$

Moreover, since $\lim_{\rho_N\to 0} A^* = 0$, we find by integration the desired expressions of A^*_0 and A'_0:

$$\frac{A^*_0}{N} = \int_0^{\rho_N} p^*_0\frac{\mathrm{d}\rho_N}{\rho_N^2} = a_1\rho_N + \tfrac{1}{2}a_2\rho_N^2 + \cdots + \tfrac{1}{8}a_8\rho_N^8$$
$$+ (a_0 - kT_0)\ln(1-a_9\rho_N)$$
$$+ kT_0\frac{(3\eta^2-4\eta)}{(1-\eta)^2}, \tag{76}$$

$$\frac{A'_0}{N} = a_1\rho_N + \tfrac{1}{2}a_2\rho_N^2 + \cdots + \tfrac{1}{8}a_8\rho_N^8$$
$$+ (a_0 - kT_0)\ln(1-a_9\rho_N). \tag{77}$$

For the density dependence of the ideal reduced internal energy and Gamma ideal reduced entropy and heat capacity, we used a simple fifth order Taylor expansion in ρ_N:

$$\frac{U^*_0}{N} = b_0\rho_N + b_1\rho_N^2 + b_2\rho_N^3 + b_3\rho_N^4 + b_4\rho_N^5, \tag{78}$$

$$\frac{S^*_{\Gamma 0}}{N} = c_0\rho_N + c_1\rho_N^2 + c_2\rho_N^3 + c_3\rho_N^4 + c_4\rho_N^5, \tag{79}$$

$$\frac{C^*_{V\Gamma 0}}{N} = d_0\rho_N + d_1\rho_N^2 + d_2\rho_N^3 + d_3\rho_N^4 + d_4\rho_N^5. \tag{80}$$

Finally, for C^*_{V0} we used a fifth order polynomial plus an additional term, in order to have a good description even at very low density:

$$\frac{C^*_{V0}}{N} = e_0\rho_N + e_1\rho_N^2 + e_2\rho_N^3 + e_3\rho_N^4 + e_4\rho_N^5$$
$$+ \exp\{-e_5(\rho_N)^{1/2}\}(e_6 - e_0)\rho_N. \tag{81}$$

In the low density range, the very low energies become more probable than the very high ones in the absence of many repulsive collisions. Hence in general for dilute fluids we can assume that the perturbation corresponds to the very low energy configurations, as indeed found for the LJ fluid. So $\Delta U_{\max}$ and γ are both negative when $\rho_N < \rho_{N_s}$ and both positive when $\rho_N > \rho_{N_s}$, where ρ_{N_s} is the 'switching' density of the perturbation. Note that when $\rho_N = \rho_{N_s}$, $\Delta U_{\max}$ and γ are not necessarily zero; in fact, for a LJ fluid $\Delta U_{\max}$ has a singularity at this density, while γ is zero. It should be clear that for $\rho_N < \rho_{N_s}$ where γ is negative, the singularity temperature $T_s = -\gamma$ should always be inside the coexistence region. This is because for each state point in ρ_N, T

Downloaded By: [EBSCOHost EJS Content Distribution] At: 14:09 25 March 2008

space outside the coexistence region the thermodynamic properties, which clearly do not diverge, are described by the perturbed Gamma state of the corresponding isochore. Since in the limit $\rho_N \to 0$ the coexistence line tends to zero as well, we must have $\lim_{\rho_N \to 0} \gamma = 0$. Hence from equation (71) follows $\lim_{\rho_N \to 0} (S_0^* - S_{\Gamma 0}^*)/(C_{V0}^* - C_{V\Gamma 0}^*) = -1/2$, and so with the density expressions of $S_0^* = (U_0^* - A_0^*)/T_0$, $S_{\Gamma 0}^*$ and $C_{V\Gamma 0}^*$ (equations (76)–(80)), we find that e_6 is given by

$$e_6 = 2c_0 + d_0 - 8v - 2[b_0 - a1 + a_9(a_0 - T_0)]/T_0. \quad (82)$$

In this way γ correctly tends to zero as $\rho_N \to 0$.

Summarizing, we model the perturbed Gamma state, either using the free energy and pressure input properties for each isochore (DD EOS), or interpolating the reference isotherm parameters with 32 coefficients (CD EOS). We report the results in section 6. For both approaches we used the hard-sphere model for the confinement, equations (70)–(72).

It is worth mentioning that, at least for the LJ fluid, the inclusion of the perturbation in the equation of state is only really necessary if we want to reproduce with high accuracy the fluid thermodynamics over a very large temperature range [23]. For a smaller temperature range an EOS, based on the confined Gamma state, corresponding to a perturbed Gamma state with $\Delta U_{\max} = \gamma = 0$, has in general a comparable accuracy, as indeed obtained for the LJ fluid when $1 \leqslant T \leqslant 6$ (data not shown).

4. Simulation data for the LJ fluid

We will apply the equation of state to the Lennard-Jones (LJ) fluid, the molecules of which interact via the following truncated and shifted pair-potential

$$u(r_{ij}) = 4\left[\left(\frac{1}{r_{ij}}\right)^{12} - \left(\frac{1}{r_{ij}}\right)^{6}\right] - 4\left[\left(\frac{1}{r_c}\right)^{12} - \left(\frac{1}{r_c}\right)^{6}\right], \quad r_{ij} \leqslant r_c, \quad (83)$$

which is zero at and beyond the cut-off distance r_c. Note that simulations with this potential, if properly performed, should give thermodynamic averages that are internally consistent, i.e. fulfil all the basic thermodynamic relations [24]. In the absence of internal degrees of freedom, the sum of these pair interactions clearly yields the ideal reduced energy U^*. Like equation (83), all results are given in the usual reduced LJ units [25]. To avoid confusion with the 'confined ideal reduced' *properties* as defined in section 2.1, the conventional '*' on the properties, to indicate that they are expressed in reduced LJ *units*, is dropped in this article. Note also that for simplicity from now on every thermodynamic property will be given as a molecular property, although not explicitly indicated. As 'experimental' data we used values obtained by molecular dynamics or Monte Carlo (MC) simulations.

Usually a long-range correction is applied to the thermodynamic averages to compensate for the use of a cut-off, assuming the radial distribution function to be unity beyond r_c. However, such long-range corrections [25] applied to the internal energy, pressure and chemical potential, are thermodynamically not completely consistent. We decided to use the 'crude' uncorrected thermodynamic data from simulations with the truncated and shifted potential, equation (83), which should be internally consistent. If wanted, the long-range (LR) and the shift corrections for the energy, pressure and chemical potential [4],

$$\Delta U^* = \Delta U_{\mathrm{LR}}^* + \Delta U_{\mathrm{shift}}^* = \tfrac{32}{9}\pi\rho_N\left[r_c^{-9} - \tfrac{3}{2}r_c^{-3}\right], \quad (84)$$

$$\Delta p = \Delta p_{\mathrm{LR}} = \tfrac{32}{9}\pi\rho_N^2\left[r_c^{-9} - \tfrac{3}{2}r_c^{-3}\right], \quad (85)$$

$$\Delta \mu = \Delta \mu_{\mathrm{LR}} + \Delta \mu_{\mathrm{shift}} = \tfrac{64}{9}\pi\rho_N\left[r_c^{-9} - \tfrac{3}{2}r_c^{-3}\right], \quad (86)$$

can be applied afterwards, as will be done in section 6.

Values in the literature (e.g. Nicolas *et al.* [5], Sun and Teja [6], Johnson *et al.* [4] and references therein) for different state points of the Lennard-Jones fluid obtained either by molecular dynamics or Monte Carlo simulations are usually restricted to the temperature range below $T = 6.0$. To be able to severely test our EOS and its ability to extrapolate to high temperature, we generated extra state points by molecular dynamics above $T = 6.0$. We used the GROMACS software package [26], with a Gaussian isokinetic temperature coupling [27, 28] that should provide a canonical distribution in configurational space [29], a leap-frog integration scheme, cut-off radius $r_c = 4.0$ and shifted potential, equation (83). After equilibration (50 000 steps), each production run consisted of 1500 000 steps, with timestep Δt given in table 1. All systems consisted of 864 atoms, except at $T = 20$, $\rho_N = 1.0$, where a system of 1728 atoms was used, as the thermodynamic averages were somewhat size dependent at these conditions. At other densities and/or temperatures both system sizes gave identical results. Values of U^* and p are given in table 1, with their estimated random error [23, 25, 30].

5. Parametrization procedure

Both the DD and CD equations were parametrized on the following simulation data.

At densities $\rho_N = 0.01$ and 0.05 ($0.95 \leqslant T \leqslant 6.0$) we used selected data from Sun and Teja [6] (28 points); at densities 0.1, 0.2, 0.3, ..., 0.9 and 1.0 ($1.0 \leqslant T \leqslant 6.0$) we used selected data from Johnson *et al.* [4] (109 points); at the latter densities for $T > 6.0$, we used the data from table 1 (50 points). The data of Sun and Teja were

Downloaded By: [EBSCOHost EJS Content Distribution] At: 14:09 25 March 2008

Table 1. Extra molecular dynamics simulation results of this work for the EOS parametrizations, using the truncated and shifted LJ potential, equation (83). Numbers between parentheses are the random errors of the mean in the last decimal place(s). No long-range or shift correction is applied to the averages.

ρ_N	T	p	U^*	Δ_t	ρ_N	T	p	U^*	Δ_t
0.1	6.0	0.651 9(2)	− 0.450 2(4)	0.002	0.6	6.0	8.593(3)	− 2.229 6(10)	0.002
0.1	8.0	0.882 8(2)	− 0.388 1(4)	0.002	0.6	8.0	11.572(4)	− 1.642 5(12)	0.002
0.1	10.0	1.111 9(2)	− 0.330 2(5)	0.000 5	0.6	10.0	14.404(5)	− 1.091 8(16)	0.000 5
0.1	12.0	1.339 3(6)	− 0.273 9(10)	0.000 1	0.6	12.0	17.131(9)	− 0.565 5(29)	0.000 1
0.1	16.0	1.792 6(8)	− 0.166 5(10)	0.000 05	0.6	16.0	22.373(19)	0.421 5(49)	0.000 05
0.1	20.0	2.243 8(10)	− 0.065 0(18)	0.000 05	0.6	20.0	27.395(7)	1.353 5(26)	0.000 05
0.2	6.0	1.450 8(5)	− 0.886 9(5)	0.002	0.7	6.0	12.549(4)	− 2.318 7(10)	0.002
0.2	8.0	1.986 5(6)	− 0.754 0(6)	0.002	0.7	8.0	16.600(4)	− 1.555 3(13)	0.002
0.2	10.0	2.516 5(7)	− 0.626 8(7)	0.000 5	0.7	10.0	20.416(5)	− 0.846 5(16)	0.000 5
0.2	12.0	3.035 3(16)	− 0.507 5(13)	0.000 1	0.7	12.0	24.034(12)	− 0.181 7(35)	0.000 1
0.2	16.0	4.067 6(24)	− 0.278 2(22)	0.000 05	0.7	16.0	31.046(19)	1.089 9(55)	0.000 05
0.2	20.0	5.089 5(13)	− 0.048 2(13)	0.000 05	0.7	20.0	37.624(22)	2.252 9(62)	0.000 05
0.3	6.0	2.485(1)	− 1.301 5(6)	0.002	0.8	6.0	18.198(5)	− 2.209 2(12)	0.002
0.3	8.0	3.421(1)	− 1.084 4(7)	0.002	0.8	8.0	23.553(6)	− 1.244 8(16)	0.002
0.3	10.0	4.336(1)	− 0.879 5(9)	0.000 5	0.8	10.0	28.577(7)	− 0.351 9(19)	0.000 5
0.3	12.0	5.235(3)	− 0.680 9(17)	0.000 1	0.8	12.0	33.305(14)	0.479 4(38)	0.000 1
0.3	16.0	6.991(5)	− 0.306 2(31)	0.000 05	0.8	16.0	42.409(25)	2.061 2(63)	0.000 05
0.3	20.0	8.716(5)	0.059 7(30)	0.000 05	0.8	20.0	50.920(27)	3.504 8(71)	0.000 05
0.4	6.0	3.879(1)	− 1.681 6(7)	0.002	0.9	6.0	26.455(6)	− 1.837 4(13)	0.002
0.4	8.0	5.337(2)	− 1.363 3(9)	0.002	0.9	8.0	33.119(7)	− 0.636 6(16)	0.002
0.4	10.0	6.751(2)	− 1.061 6(11)	0.000 5	0.9	10.0	39.595(8)	0.465 8(19)	0.000 5
0.4	12.0	8.131(4)	− 0.769 0(20)	0.000 1	0.9	12.0	45.648(16)	1.484 4(35)	0.000 1
0.4	16.0	10.811(8)	− 0.217 7(37)	0.000 05	0.9	16.0	57.255(27)	3.413 3(64)	0.000 05
0.4	20.0	13.426(4)	0.314 4(21)	0.000 05	0.9	20.0	68.032(33)	5.166 6(79)	0.000 05
0.5	6.0	5.788(2)	− 1.998 4(9)	0.002	1.0	6.0	37.253(7)	− 1.104 9(15)	0.002
0.5	8.0	7.957(3)	− 1.560 5(10)	0.002	1.0	8.0	46.122(9)	0.349 4(20)	0.002
0.5	10.0	9.997(3)	− 1.146 4(12)	0.000 5	1.0	10.0	54.252(9)	1.695 9(21)	0.000 5
0.5	12.0	11.975(7)	− 0.746 2(27)	0.000 1	1.0	12.0	62.131(20)	2.949 87(45)	0.000 1
0.5	16.0	15.818(11)	0.014 6(40)	0.000 05	1.0	16.0	76.412(34)	5.226 4(78)	0.000 05
0.5	20.0	19.501(5)	0.722 6(22)	0.000 05	1.0	20.0	89.995(27)	7.339 0(60)	0.000 05

recorrected to obtain truncated-and-shifted potential values.

The CD equation was parametrized in the following way. Since it is highly nonlinear in the coefficients a_i, b_i, c_i, d_i, e_i and parameter v, an overall fit to the data at once was impossible. We therefore adopted the following strategy:

(1) First, the pressure p_0 was fitted at the reference isotherm $T_0 = 2.0$ by equation (73), obtaining in this way the coefficients a_i and also the density expression of A_0' (equation (77)). Also the energy U_0^* along the reference isotherm was fitted by equation (78), yielding the coefficients b_i.

(2) The value of v, the hard-sphere volume, was evaluated in the following way. At each of the 12 isochores, the experimental energy U^* was fitted by the expression of $U^*(T)$ for the perturbed Gamma state, given by equations (47) and (25):

$$U^*(T; U_{\Gamma 0}^*, C_{V\Gamma 0}^*, \delta_0, \Delta U_{\max}, \gamma) = U_{\Gamma 0}^* + (T - T_0)\frac{T_0 C_{V\Gamma 0}^*}{T(1-\delta_0) + T_0\delta_0} + \frac{\Delta U_{\max} T^2}{(T+\gamma)^2}, \quad (87)$$

yielding an estimate of the five parameters $U_{\Gamma 0}^*$, $C_{V\Gamma 0}^*$, δ_0, $\Delta U_{\max}$ and γ at each density. Using these estimates, the corresponding values of the free energy $A_0^* = A_{\Gamma 0}^* + \Delta U_{\max} T_0/(T_0 + \gamma)$, equations (46) and (26), were evaluated. Since from the pressure fit already the coefficients a_i and hence the density dependence of A_0' were known, the term $k \ln \varepsilon$ could be evaluated at every density via equation (11) as

$$k \ln \varepsilon = (A_0^* - A_0')/T_0. \quad (88)$$

Downloaded By: [EBSCOHost EJS Content Distribution] At: 14:09 25 March 2008

These values were then fitted by equation (70), yielding v and the explicit density dependence of $k \ln \varepsilon$ and ξ via equations (70)–(72), and the density dependence of A_0^* from equation (76).

(3) Since already the density dependence of three of the six parameters of the isochore expression of $A'(T)$ were defined, we could eliminate 2 of the 5 parameters in the isochore expression of $U^*(T)$ at will, by expressing them in terms of the other remaining three parameters. We decided to eliminate $U_{\Gamma 0}^*$ and $\Delta U_{\max}$, yielding

$$U^*(T; C_{V\Gamma 0}^*, \delta_0, \gamma) = U_0^* + (T - T_0)\frac{T_0 C_{V\Gamma 0}^*}{T(1-\delta_0) + T_0\delta_0} + T_0\left[C_{V\Gamma 0}^*\left\{\frac{1}{\delta_0} + \frac{1}{\delta_0^2}\ln(1-\delta_0)\right\} - S_0^*\right] \times \left[\frac{T^2}{T_0\gamma}\left(\frac{T_0+\gamma}{T+\gamma}\right)^2 - \frac{T_0}{\gamma}\right], \quad (89)$$

where the values of U_0^* and $S_0^* = (U_0^* - A_0^*)/T_0$ are given by the polynomial expressions in ρ_N. This equation was used to refit U^* along each of the 12 isochores, obtaining new values of $C_{V\Gamma 0}^*$, δ_0 and γ at those densities.

(4) Next, $C_{V\Gamma 0}^*$ and δ_0, converted into $S_{\Gamma 0}^*$ via

$$S_{\Gamma 0}^* = C_{V\Gamma 0}^*\left\{\frac{1}{\delta_0} + \frac{1}{\delta_0^2}\ln(1-\delta_0)\right\} \quad (90)$$

were fitted by equations (79) and (80).

(5) Eliminating all parameters but γ in the expression of $U^*(T)$, we again refitted the energy values along each isochore to the following equation to obtain new values of γ at each density:

$$U^*(T; \gamma) = U_0^* + (T - T_0)\frac{T_0 C_{V\Gamma 0}^*}{T(1-\delta_0) + T_0\delta_0} + T_0\left[S_{\Gamma 0}^* - S_0^*\right] \times \left[\frac{T^2}{T_0\gamma}\left(\frac{T_0+\gamma}{T+\gamma}\right)^2 - \frac{T_0}{\gamma}\right], \quad (91)$$

where the values of U_0^*, S_0^*, $S_{\Gamma 0}^*$ and $C_{V\Gamma 0}^*$ are given by the polynomial expressions in ρ_N, and δ_0 is obtained from $S_{\Gamma 0}^*$ and $C_{V\Gamma 0}^*$ via equation (64).

(6) Finally, γ was converted to C_{V0}^* via

$$C_{V0}^* = C_{V\Gamma 0}^* + \frac{2T_0(S_{\Gamma 0}^* - S_0^*)}{T_0 + \gamma} \quad (92)$$

at each of the 12 densities and fitted by equation (81), including the constraint on the zero density limit of γ (equation (82)). In this iterative way all the 32 independent coefficients were obtained.

For the DD equation we used the estimates of v and the free energy input properties as described in step (2) above. In addition, we also evaluated the pressure input properties p_0', $\partial p_0'/\partial T$, $\partial^2 p_0'/\partial T^2$, $\mathrm{d}\Delta U_{\max}/\mathrm{d}V$ and $\mathrm{d}\gamma/\mathrm{d}V$ from a fit of the isochore pressure data with equation (50) and ξ provided by the value of v.

6. Results and comparison

To test the stability of the parametrization procedure described above and the ability of the QGE equations of state to extrapolate to unknown state points, the parametrization was performed on two datasets:

(a) all energy values of the dataset described in section 5 in the range $T \leqslant 20.0$ (187 points), and
(b) only energy values in the range $T \leqslant 6.0$ (137 points).

The final coefficients obtained for the CD equation using dataset A ($T \leqslant 20.0$) are given in table 2, and the equation based on this set will be referred to as 'QGE-A', the corresponding DD equation as 'dQGE-A'. The CD equation based on dataset B with $T \leqslant 6$, the coefficients of which are given in table 3, will be referred to as 'QGE-B', the corresponding DD equation as 'dQGE-B'. Note that the value of v, the hard-sphere volume per molecule, evaluated using a perturbed Gamma state model over a large density and temperature range as reported in tables 2 and 3, is very similar to the value $v \sim 0.19$ obtained by Roccatano *et al.* [23] at a single isochore using a pure confined Gamma state model in a smaller temperature range ($1.4 \leqslant T \leqslant 10$).

In order to have an overall estimate of the accuracy of the different equations of state, we calculated several statistical properties. First, we evaluated the value of χ^2 per degree of freedom, defined as

$$\chi^2/N_{\mathrm{df}} = \frac{1}{N_{\mathrm{df}}}\sum_i^{N_{\mathrm{data}}}\left(\frac{X_{i,\mathrm{EOS}} - X_{i,\mathrm{exp}}}{\sigma_{X_{i,\mathrm{exp}}}}\right)^2, \quad (93)$$

where X stands for energy and pressure, $\sigma_{X_{i,\mathrm{exp}}}$ is the experimental error (standard deviation), and $N_{\mathrm{df}} = N_{\mathrm{data}} - N_{\mathrm{par}}$ is the number of degrees of freedom, with N_{par} the number of coefficients of the EOS which were fitted on the energy and pressure data. Secondly, we calculated partial χ^2 values, defined as

$$\chi_X^2/N_{\mathrm{data}} = \frac{1}{N_{\mathrm{data}}}\sum_i^{N_{\mathrm{data}}}\left(\frac{X_{i,\mathrm{EOS}} - X_{i,\mathrm{exp}}}{\sigma_{X_{i,\mathrm{exp}}}}\right)^2, \quad (94)$$

Downloaded By: [EBSCOHost EJS Content Distribution] At: 14:09 25 March 2008

Table 2. The 32 independent coefficients of the CD perturbed Gamma equation of state QGE-A in equations (70)–(71) and equations (76)–(81) for the density dependence of the six parameters A_0^*, U_0^*, C_{V0}^*, $S_{\Gamma 0}^*$, $C_{V\Gamma 0}^*$ and ε at isotherm $T_0 = 2.0$, based on dataset A ($1.0 \leqslant T \leqslant 20$). The value of v corresponds to a hard-sphere diameter $\sigma_{HS} = 0.714\,15$. All coefficients are in reduced units.

i	a_i	b_i	c_i	d_i	e_i
0	− 57.772 381	− 6.766 771 269	− 0.886 540 024	0.240 264 838	2.772 820 359
1	201.854 809	3.575 787 554	− 1.455 723 780	0.649 393 609	− 4.436 228 538
2	− 678.012 949	− 5.960 266 536	1.326 099 535	− 0.997 026 117	3.024 514 616
3	2055.563 845	2.477 668 433	− 1.694 656 701	1.379 970 366	2.423 913 956
4	− 4891.944 123	1.896 517 395	0.658 283 266	− 0.598 175 645	− 2.026 140 177
5	8153.995 69				1.132 779 811
6	− 8577.929 95				0.912 564 161
7	5059.186 825				
8	− 1263.124 319		$v = 0.190\,705$		
9	− 3.423 831 5				

Table 3. The 32 independent coefficients of the CD perturbed Gamma equation of state QGE-B, based on dataset B ($1.0 \leqslant T \leqslant 6$).

i	a_i	b_i	c_i	d_i	e_i
0	− 57.772 381	− 6.766 771 269	− 0.872 956 488	0.235 283 471	1.765 739 772
1	201.854 809	3.575 787 554	− 1.928 774 403	1.016 658 808	− 3.773 464 278
2	− 678.012 949	− 5.960 266 536	3.213 196 979	− 2.500 157 643	3.215 568 161
3	2055.563 845	2.477 668 433	− 4.600 892 408	3.675 244 314	1.595 198 541
4	− 4891.944 123	1.896 517 395	2.049 665 016	− 1.690 310 341	− 1.576 624 871
5	8153.995 69				2.498 445 686
6	− 8577.929 95				0.934 749 866
7	5059.186 825				
8	− 1263.124 319		$v = 0.190\,705$		
9	− 3.423 831 5				

with X either energy or pressure. Thirdly, we evaluated the root mean square deviations (RMSD) as well as the % AAD of U^* and p, the latter defined as

$$\text{AAD } X = \frac{1}{N_{\text{data}}} \sum_{i}^{N_{\text{data}}} \left| \frac{X_{i,\text{EOS}} - X_{i,\text{exp}}}{X_{i,\text{exp}}} \right|, \qquad (95)$$

where X is energy or pressure.

To compare the equations of state in different temperature ranges, we used five different sets of simulation data for the calculation of the statistics.

(1) All data of Johnson *et al.* in the range $0.005 \leqslant \rho_N \leqslant 1.0$ and $0.75 \leqslant T \leqslant 2.0$, a total of 121 values of U^* (59 of which were used for the regression of our CD and DD equations) and 121 of p (59 of which were used for the regression of the DD equations).
(2) The selected energy data of Johnson *et al.* that were used for the parametrization of the QGE equations of state, in the range $0.1 \leqslant \rho_N \leqslant 1.0$ and $1.0 \leqslant T \leqslant 6.0$ (109 values), and the corresponding 109 pressure values.
(3) Set (2) augmented with values of table 1 for $T \leqslant 12.0$, in total 149 energy and 149 pressure values.
(4) Set (2) augmented with all values of table 1, in total 169 energy and 169 pressure values.
(5) The values of Miyano [31] in the temperature range $20 \leqslant T \leqslant 50$ (15 energy and 15 pressure values).

Values of χ^2/N_{df}, the partial χ^2 values, RMSD and % AAD are given in tables 4 and 5 for the two DD equations (dQGE-A and dQGE-B), the two CD equations (QGE-A and QGE-B), the MBWR equations of Johnson *et al.* [4] (MBWR-1) and Sun and Teja [6] (MBWR-2), and the equations of Kolafa and Nezbeda [7] (KN) and Mecke *et al.* [8] (VDW).

Since Johnson *et al.* and Sun and Teja used the first five virial coefficients to obtain five of the 32 linear coefficients of the MBWR equation, the number of degrees of freedom for χ^2 is $N_{\text{df}} = N_{\text{data}} - 27$ in their case. Kolafa and Nezbeda fitted 20 coefficients, hence $N_{\text{df}} = N_{\text{data}} - 20$, and Mecke *et al.* evaluated 32 coefficients based on energy and pressure data, so

Downloaded By: [EBSCOHost EJS Content Distribution] At: 14:09 25 March 2008

Table 4. Values of χ^2/N_{df} (equation (93)), and partial χ^2 (equation (94)), root mean square deviations and % AAD (equation (95)) of U^* and p, using three different datasets, see text, for different equations of state parametrized in the range $T \leqslant 6$.

Dataset	T range		dQGE-B	QGE-B	MBWR-1	MBWR-2
(1)	$0.75 \leqslant T \leqslant 2.0$	χ^2/N_{df}	10.3	25.2	22.5	89.5
		$\chi^2_{U^*}/N_{data}$	4.0	13.6	36.9	100.2
		RMSD U^*	0.005	0.008	0.011	0.021
		% AAD U^*	0.32%	0.67%	0.75%	1.43%
		χ^2_p/N_{data}	6.5	30.1	3.0	58.8
		RMSD p	0.014	0.051	0.009	0.068
		% AAD p	2.27%	2.64%	1.18%	2.53%
(2)	$1.0 \leqslant T \leqslant 6.0$	χ^2/N_{df}	2.3	32.4	43.0	251.8
		$\chi^2_{U^*}/N_{data}$	0.8	3.0	70.2	133.5
		RMSD U^*	0.002	0.005	0.027	0.028
		% AAD U^*	0.08%	0.20%	0.71%	1.22%
		χ^2_p/N_{data}	1.7	52.3	5.2	307.7
		RMSD p	0.005	0.082	0.019	0.194
		% AAD p	0.17%	0.92%	0.82%	1.76%
(3)	$1.0 \leqslant T \leqslant 12.0$	χ^2/N_{df}	352.2	119.5	5 930	2 915
		$\chi^2_{U^*}/N_{data}$	282.4	79.1	10 799	4 466
		RMSD U^*	0.031	0.021	0.253	0.140
		% AAD U^*	2.05%	1.29%	13.42%	7.39%
		χ^2_p/N_{data}	185.7	134.2	145.8	914.8
		RMSD p	0.13	0.11	0.11	0.25
		% AAD p	0.28%	0.76%	0.77%	1.54%

Table 5. Values of χ^2/N_{df} (equation (93)), and partial χ^2 (equation (94)), root mean square deviations and % AAD (equation (95)) of U^* and p, using three different datasets, see text, for different equations of state roughly parametrized in the range $T \leqslant 20$.

Dataset	T range		dQGE-A	QGE-A	KN	VDW
(1)	$0.75 \leqslant T \leqslant 2.0$	χ^2/N_{df}	38.3	47.3	4.0	2.4
		$\chi^2_{U^*}/N_{data}$	36.4	47.5	5.0	2.9
		RMSD U^*	0.011	0.011	0.005	0.003
		% AAD U^*	0.39%	0.70%	0.56%	0.54%
		χ^2_p/N_{data}	2.7	34.6	2.0	1.2
		RMSD p	0.011	0.054	0.010	0.008
		% AAD p	1.18%	2.38%	1.48%	0.88%
(4)	$1.0 \leqslant T \leqslant 20.0$	χ^2/N_{df}	16.3	96.2	25.1	25.3
		$\chi^2_{U^*}/N_{data}$	4.0	6.0	13.3	17.4
		RMSD U^*	0.004	0.005	0.013	0.018
		% AAD U^*	0.36%	0.83%	0.92%	1.18%
		χ^2_p/N_{data}	19.0	168.2	32.3	28.4
		RMSD p	0.03	0.20	0.06	0.06
		% AAD p	0.34%	0.73%	0.57%	0.41%
(5)	$20.0 \leqslant T \leqslant 50.0$	χ^2/N_{data}	0.6	1.8	0.6	0.6
		$\chi^2_{U^*}/N_{data}$	0.8	0.8	1.0	0.7
		RMSD U^*	0.33	0.33	0.30	0.35
		% AAD U^*	15.54%	15.35%	17.11%	13.19%
		χ^2_p/N_{data}	0.3	2.8	0.3	0.6
		RMSD p	0.66	1.98	0.46	0.77
		% AAD p	0.65%	0.88%	0.50%	0.82%

Downloaded By: [EBSCOHost EJS Content Distribution] At: 14:09 25 March 2008

$N_{df} = N_{data} - 32$. For the two CD QGE equations (QGE-A and QGE-B) we have 32 nonlinear coefficients, hence $N_{df} = N_{data} - 32$. Finally, for the two DD QGE equations (dQGE-A and dQGE-B) we have 10 parameters per isochore, hence $N_{df} = N_{data} - 100$.

As previously discussed [23], for a LJ fluid a simulation of a few million time-steps seems to provide virtually 'exact' thermodynamic averages as shown by the extremely small estimated random errors, see table 1. In such a condition even an excellent model will have significant deviations with respect to the experimental properties. Therefore the χ^2 and partial χ^2 values give a measure of the physical accuracy of the model itself with respect to the 'exact' system behaviour, and hence can only be used for a relative comparison between different models.

The results for the equations of state which were parametrized in the temperature range $T \leqslant 6$ are summarized in table 4.

First of all it is clear that both QGE equations are very accurate within their parametrization range ($1.0 \leqslant T \leqslant 6.0$). Especially the dQGE-B equation is very accurate for both energy and pressure and the accuracy for the energy is about the same for dQGE-B and QGE-B. The pressure is for the latter somewhat less accurate, obviously since in that case almost no pressure data were used in the regression. Comparing with the Johnson *et al.* MBWR-1 equation, we see that the dQGE-B equation is clearly superior and the QGE-B is on average comparable (χ^2 values), with less accuracy for the pressure and higher accuracy for the energy ($\chi^2_{U^*}$, RMSD and %AAD U^*). The MBWR-2 equation is in general worse than both QGE equations of state.

In the range $0.75 \leqslant T \leqslant 2.0$, including many low-temperature data which were not used to regress the QGE equations of state, we have a similar situation. The dQGE-B equation is clearly superior, and the QGE-B and MBWR-1 equations are on average comparable, although the QGE-B describes the energy better.

If we extrapolate in temperature up to twice the parametrization range, we see that both QGE equations are still very accurate compared to the MBWR equations, especially for the energy. Curiously, the QGE-B equation is better than the dQGE-B, probably because some small local noise in the parameters in the range up to $T = 6$ is smoothed in the QGE-B equation by the interpolation polynomials. It is clear that with both QGE equations of state it is possible to extrapolate in temperature to at least twice the parametrization range with good accuracy. The polynomial description of the MBWR equations does not guarantee a reasonable behaviour outside its parametrization range. Since we almost did not use pressure data for the regression of the QGE-B equation, the good reproduction of the pressure data by this equation of state is therefore a more independent and relevant test.

The results for the equations of state which were parametrized roughly in the range up to $T = 20$ are summarized in table 5.

First of all we see also here that the main difference between the dQGE-A and QGE-A equations is the accuracy of the pressure. This property is reproduced very accurately by the DD equation, and fairly accurately by the CD equation, where basically no pressure data were used for the regression. The use of interpolation polynomials for the input properties at T_0 obviously does not alter much the precision of the energy values.

In the range $1.0 \leqslant T \leqslant 20.0$ all equations are basically comparable for the energy, and for the pressure the dQGE-A, KN and VDW equations are roughly comparable, although the dQGE-A is slightly better for both energy and pressure. It should be considered that although we did not use pressure data for the QGE-A equation, the average absolute error in the pressure is still only 0.73%.

In the low temperature range, $0.75 \leqslant T \leqslant 2.0$, both KN and VDW equations are very accurate for both energy and pressure, and the pressure accuracy of the dQGE-A is comparable. The energy of the QGE equations is still fairly accurate, but for this range less precise. It must be stressed that both KN and VDW equations were fitted using much more data points in this range than both QGE equations.

Finally, also for these equations we looked at extrapolations in the temperature range $20 \leqslant T \leqslant 50$, comparing with the data of Miyano [31]. We see that all equations have comparable accuracy in this range, and only the pressure is, as usual, somewhat less precisely reproduced by the QGE-A equation. Note that Mecke *et al.* used data up to $T = 100$ to improve the high temperature behaviour of their empirical polynomial. However, considering the extremely large temperature range the accuracy of all equations is still rather high.

Summarizing, we see that the QGE theory at the level of the perturbed confined Gamma state is perfectly capable of describing the thermodynamics of a simulated model fluid, in this case the Lennard-Jones fluid, with high accuracy. Moreover, because of their theoretical basis, the QGE equations are able to extrapolate in temperature to at least twice the parametrization range with reasonable accuracy. If we use for the parametrization the same information as the most successful EOS up to now (i.e. both energy and pressure data), the DD QGE equations (dQGE-A and B) are at least comparable to the KN and VDW equations and better than the MBWR equations. If we only use energy data for the regression and apply simple interpolation polynomials in density (QGE-A and B), we still have a very accurate

Downloaded By: [EBSCOHost EJS Content Distribution] At: 14:09 25 March 2008

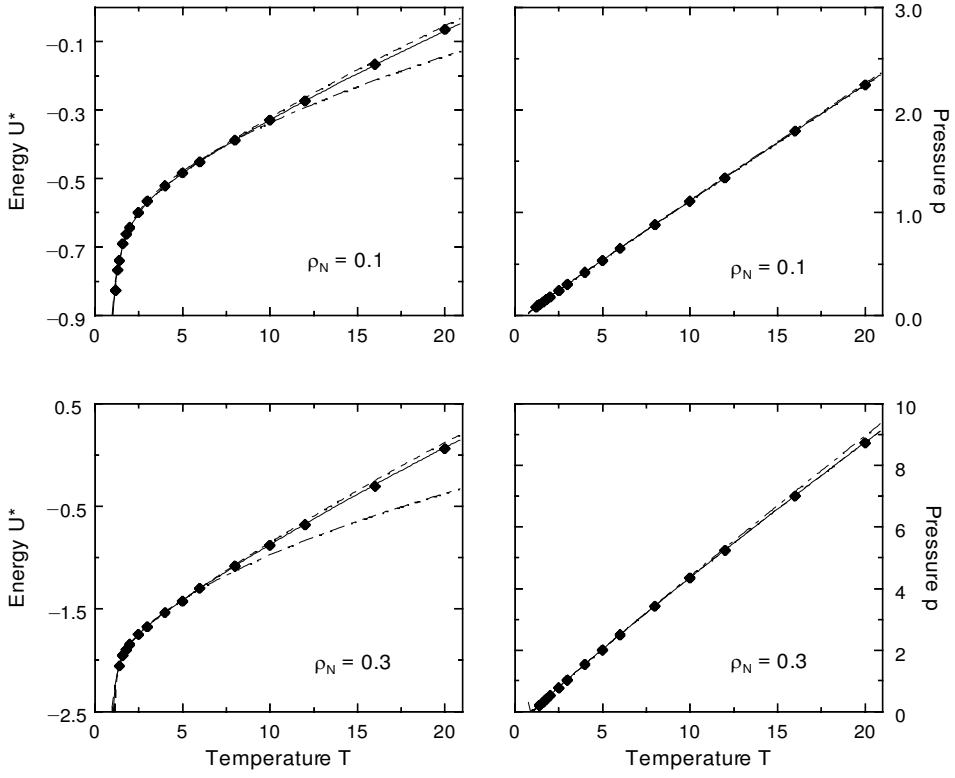

Figure 2. Energy U^* and pressure p of the LJ fluid for densities $\rho_N = 0.1$ and 0.3. Legend: simulation data (◆), QGE-A equation of state (——), QGE-B equation of state (– – –) and MBWR-1 equation of state [4] (- ' - ' -).

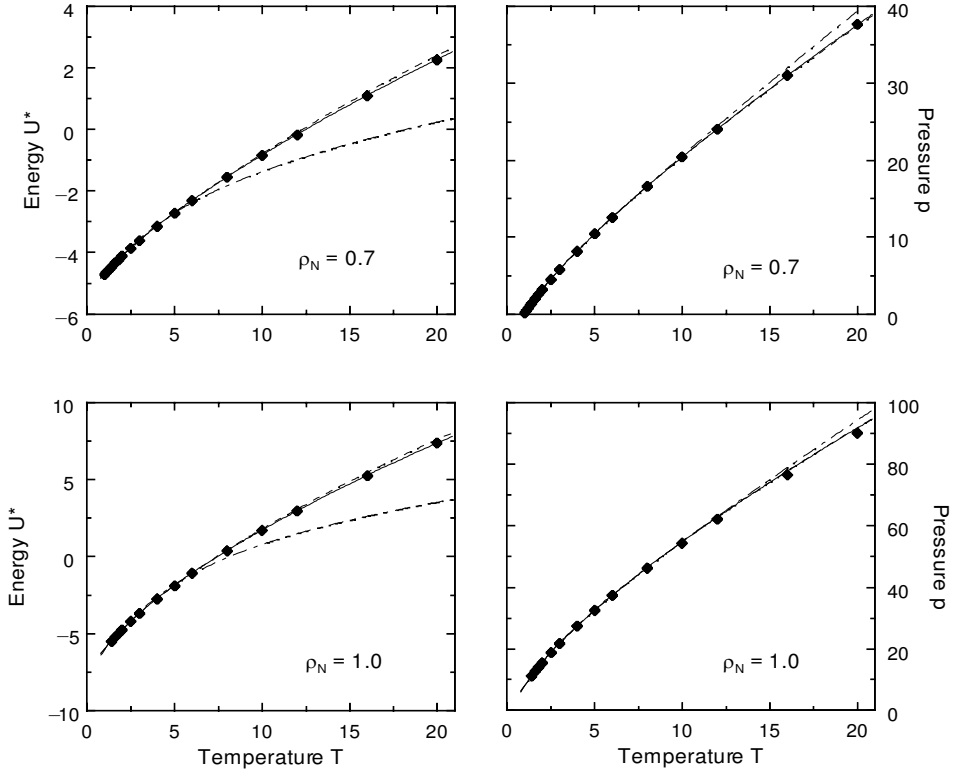

Figure 3. Energy U^* and pressure p of the LJ fluid for densities $\rho_N = 0.7$ and 1.0. Legend: simulation data (◆), QGE-A equation of state (——), QGE-B equation of state (– – –) and MBWR-1 equation of state [4] (- ' - ' -).

Downloaded By: [EBSCOHost EJS Content Distribution] At: 14:09 25 March 2008

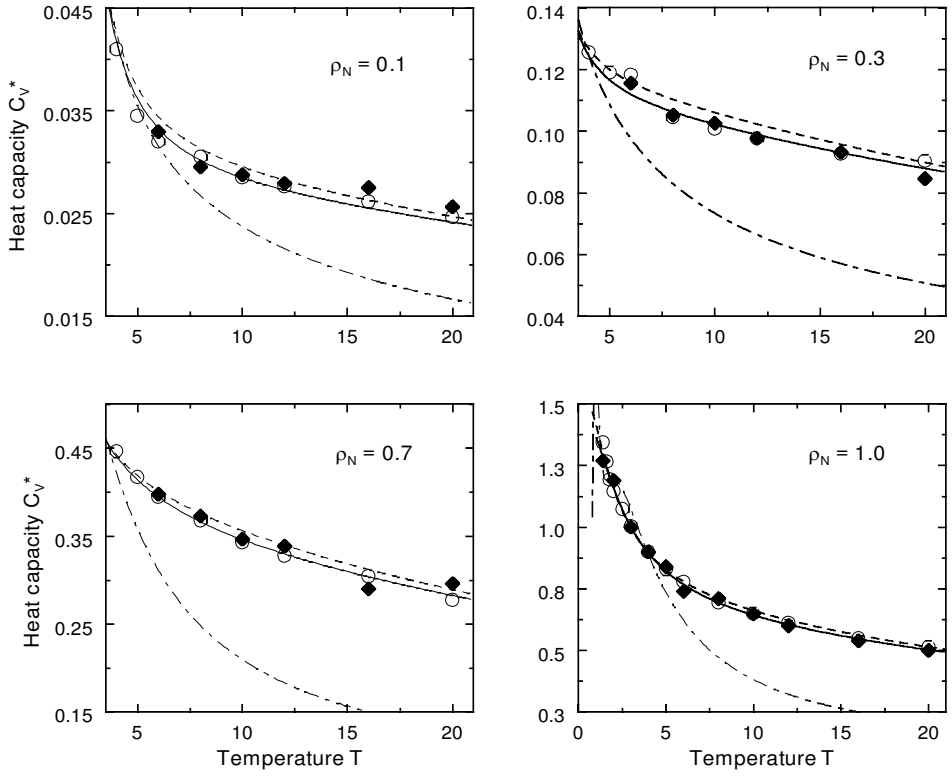

Figure 4. Isochoric heat capacity C_V^* of the LJ fluid for densities $\rho_N = 0.1$ 0.3, 0.7 and 1.0. Legend: simulation data, based on M_2 (◆) and numerical derivative of U^* (○), QGE-A equation of state (——), QGE-B equation of state (– – –) and MBWR equation of state [4] (- ' - ' -).

description of the energy and a fairly accurate description of the pressure, even if we extrapolate outside the parametrization range. Interestingly, the value of v and hence of $\sigma_{HS} \sim 0.71$, obtained for both $T \leqslant 6$ and $T \leqslant 20$ ranges, still gives a very accurate description at $T = 50$ (i.e. ~ 37 times T_c), while σ_{HS} in the KN equation, for example, changes from 1.02 ($T = 1.0$) to 0.82 ($T = 50$).

In the rest of this results section we will focus on the properties of the two CD equations of state, i.e. the QGE-A and QGE-B equations.

In figures 2 and 3 the 'experimental' simulation data of U^* and p are shown at densities $\rho_N = 0.1$, 0.3, 0.7 and 1.0, along with the predictions of the QGE-A and QGE-B equations of state. As can be seen from the figures, in accordance with tables 4 and 5, the QGE-A equation reproduces in an excellent way the simulation data in the whole temperature range for all densities. Also the QGE-B equation shows very good agreement, although slightly worse outside its parametrization range. For comparison, the MBWR-1 equation of state of Johnson *et al.* is also shown, which clearly deviates strongly for the energy outside its parametrization range.

To severely test the (physical) quality of the QGE equations of state, we also looked at a higher order derivative of the free energy or pVT surface, the heat capacity C_V^*, which is a very sensitive property. We compared the different equations of state with simulation data, as well as two different ways to evaluate C_V^* from simulations.

In figure 4 the heat capacity, calculated as the numerical derivative of U^*, is plotted together with the predictions of the QGE-A, QGE-B and MBWR-1 equations. While the first two equations give almost identical results and agree very well with the experimental values, the latter EOS is clearly off, already below $T = 6$. In tables 6 and 7 we give the partial χ^2 values for the various equations of state in different tempera-

Table 6. Values of $\chi^2_{C_V^*}/N_{\text{data}}$ (equation (94)), using three different datasets, for different equations of state parametrized in the range $T \leqslant 6$.

Dataset	T range		dQGE-B	QGE-B	MBWR-1	MBWR-2
(1)	$0.75 \leqslant T \leqslant 2.0$	$\chi^2_{C_V^*}/N_{\text{data}}$	1.2	2.5	11.7	13.6
(2)	$1.0 \leqslant T \leqslant 6.0$	$\chi^2_{C_V^*}/N_{\text{data}}$	1.8	2.0	126.7	64.6
(3)	$1.0 \leqslant T \leqslant 12.0$	$\chi^2_{C_V^*}/N_{\text{data}}$	97.7	16.9	2538	702.9

Downloaded By: [EBSCOHost EJS Content Distribution] At: 14:09 25 March 2008

Table 7. Values of $\chi^2_{C_V^*}/N_{\text{data}}$ (equation (94)), using two different datasets, for different equations of state parametrized in the range $T \leqslant 20$.

Dataset	T range		dQGE-A	QGE-A	KN	VDW
(1)	$0.75 \leqslant T \leqslant 2.0$	$\chi^2_{C_V^*}/N_{\text{data}}$	2.2	2.9	2.2	1.6
(4)	$1.0 \leqslant T \leqslant 20.0$	$\chi^2_{C_V^*}/N_{\text{data}}$	2.8	3.2	3.6	5.9

ture ranges. Note that since we had to evaluate C_V^* numerically from U^* data, the C_V^* set for $0.75 \leqslant T \leqslant 2.0$ contains slightly less data than the corresponding energy and pressure sets. Table 6 provides a comparison between the equations which were parametrized in the range $T \leqslant 6$. In all cases and especially for the extrapolation range both QGE equations are superior to the MBWR equations, as already clear from figure 4. In accordance with the energy statistics (table 4), the extrapolation of the CD equation is better than the DD one. The EOS parametrized roughly in the range $T \leqslant 20$ are compared in table 7. They all have a comparable accuracy and in the range $1.0 \leqslant T \leqslant 20.0$ the QGE equations are slightly better than the VDW equation. Clearly, the QGE equations of state also provide a good description of higher order free energy derivatives.

To test the simulation procedure, following Roccatano *et al.* [23], we also evaluated C_V^* via the second central moment (the variance) of the overall potential energy from the simulation, using the general statistical mechanical relation [18, 25, 32, 33]

$$C_V^* = \frac{\langle (\mathcal{U} - U^*)^2 \rangle}{kT^2}. \tag{96}$$

As is well known, fluctuations are much more affected by the simulation details (integration algorithm, time-step, temperature coupling, cut-off, periodic boundary conditions, system size etc.) than the usual thermodynamic averages. Using appropriate values though for the time-step, runlength, system size and cut-off radius, combined with a rigorous temperature coupling, it is obvious from figure 4 that the potential energy fluctuations provide values of C_V^* which are fairly close to the numerical derivatives of U^*, in most cases within 2σ of C_V^* evaluated by equation (96). This shows that even up to the level of second order fluctuations, our NVT molecular dynamics simulations are thermodynamically rather consistent. Moreover, such a result confirms in an independent way the physical correctness of the QGE equations of state.

We also calculated the coexistence line for the *full* LJ potential, by equating the gas and liquid pressures $p = p' + \rho_N kT$ and chemical potentials $\mu = A'/N + p'/\rho_N + kT \ln(\rho_N)$, including the correction terms (equations (85) and (86)). The results are given in figures 5 and 6 for the QGE-A and B equations, together with data from simulations and some integral equations.

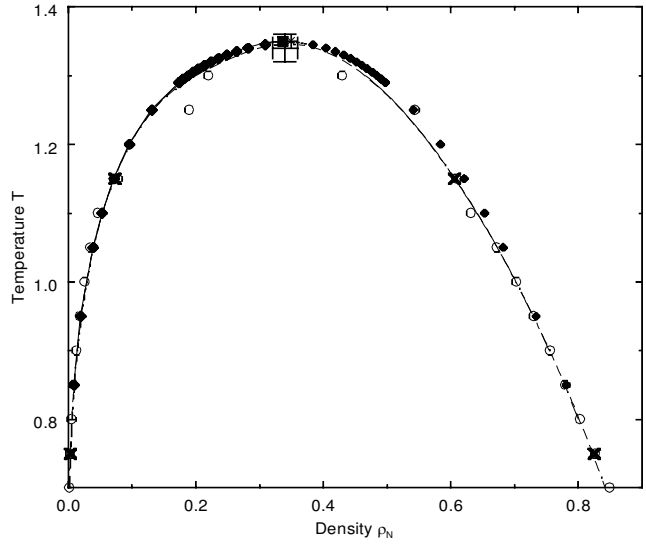

Figure 5. Liquid–vapour coexistence line of the LJ fluid. Legend: QGE-A equation of state adding long-range and shift corrections to μ and p (——), QGE-B EOS (– – –), simulation results from Hansen and Verlet [34] (×), Adams [35], $T \leqslant 1.1$, and Adams [36], $T \geqslant 1.15$, (○), and OCT data from Sung and Chandler [37] (◆). The critical point of the QGE-A equation is indicated by ■, the one estimated by Verlet [38] by +, and the one imposed by Nicolas *et al.* [5] by an asterisk (*).

Both QGE equations of state yield almost identical coexistence lines, which correspond very well with the NVT results of Hansen and Verlet [34], figure 5, and the optimized cluster theory (OCT) calculations of Sung and Chandler [37]. Also the lower temperature results of Adams [35], using a combination of NVT and μVT MC and EOS, are in good agreement, although his high temperature results [36], using μVT MC, show a somewhat strange behaviour, see also [39].

In figure 6 we compare the two QGE coexistence lines with the results of Gibbs ensemble (GE) simulations of Panagiotopoulos [40], Panagiotopoulos *et al.* [41] and Smit and Frenkel [42], and the $NpT+$ test particle results of Lotfi *et al.* [39]. Clearly, up to $T = 1.25$ the simulations and QGE predictions agree very well, and only at

Downloaded By: [EBSCOHost EJS Content Distribution] At: 14:09 25 March 2008

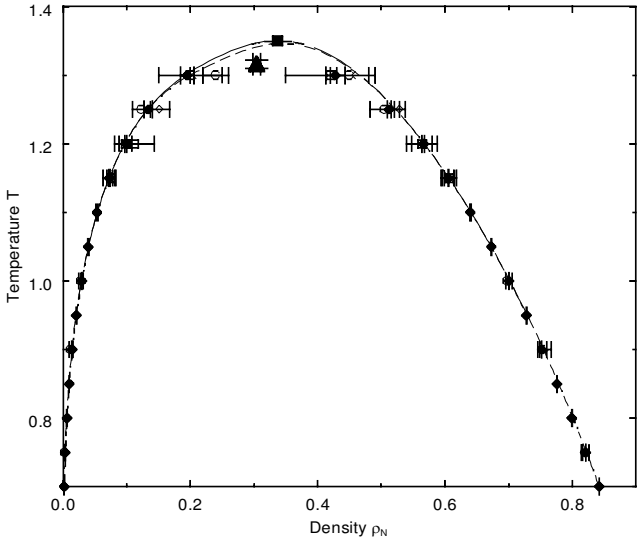

Figure 6. Liquid–vapour equilibrium pressure of the LJ fluid. Legend: QGE-A EOS (——), QGE-B EOS (– – –), *NpT* simulations of Lotfi *et al.* [39] (◆) and Gibbs ensemble simulation results from Panagiotopoulos [40] (○), Panagiotopoulos *et al.* [41] (◇) and Smit and Frenkel [42] (□). The critical point from the QGE-A equation is indicated by ■, the one estimated by Smit [24] by ▲.

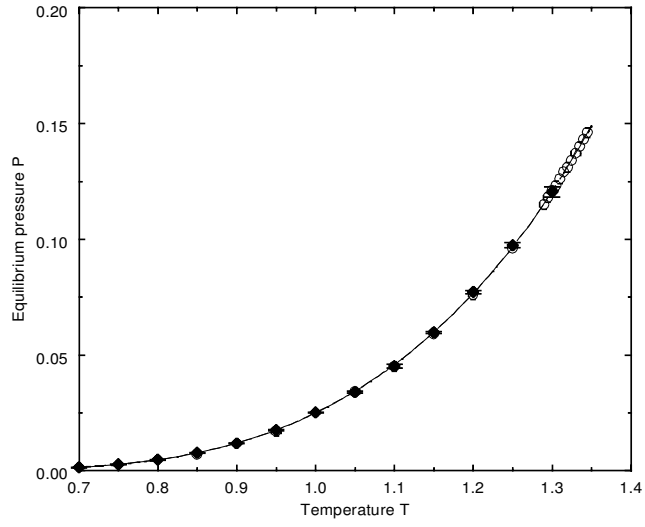

Figure 7. Liquid–vapour equilibrium pressure of the LJ fluid. Legend: QGE-A EOS with long-range and shift corrections (——), QGE-B EOS (– – –), OCT data from Sung and Chandler [37] (○) and values from Lotfi *et al.* [39] (◆).

$T = 1.3$, the highest temperature where simulation data are available, there is some discrepancy, although the QGE curves are still within the (rather large) errorbars of most GE data.

In figure 7 we present the equilibrium pressure along the coexistence line for both QGE equations (which on the scale of the figure are identical), and the values of Sung and Chandler [37] and Lotfi *et al.* [39]. Clearly, all values agree very well with the QGE predictions.

The values of the critical point based on the QGE equations of state are given in table 8, together with a summary of other estimates, based on various simulations, equations of state and integral equations. Other estimates based on integral equations can be found in [43] and [45], and give a similar picture.

Our values are very similar to the OCT results of Sung and Chandler [37] and to the results of Levesque and Verlet [44], using two different EOS based on their *NVT* MC data. Also the Percus–Yevick II (PY II) results of Verlet and Levesque [43] are very close, and our values and the values imposed by Nicolas *et al.* [5] for their MBWR equation lay within Verlet's estimate [38] of the critical point based on the PY II equation in combination with *NVT* MD data. The critical point obtained from the KN equation [7] is also very close.

The data of the Gibbs ensemble MC or *NpT* MD simulations, which are fitted to a scaling law for the density with critical exponent $\beta \sim 1/3$, either or not in combination with the law of rectilinear diameters [46], result in a critical temperature and density that are lower than estimates based on *NVT* simulations or integral equations. This is usually attributed to the fact that (large) density fluctuations, which are to occur close to the critical point, are suppressed in both *NVT* simulations and in integral equations [34, 37, 44], while the Gibbs ensemble procedure in principle does allow large fluctuations [47].

However, from figure 6 it seems that in the whole range where GE or *NpT* data are available there is hardly any difference with our EOS coexistence line. This suggests that a large effect on the critical point discrepancy is due to the 'extrapolation' procedure used by these authors [24, 36, 39]. They actually fitted the direct coexistence data ($T \leqslant 1.30$) with a macroscopic scaling law usually imposing a value of the critical exponent β close to 1/3. Interestingly, Adams [36] remarks that the critical temperature within his simulations should be between 1.30 and 1.35, while the estimate from the scaling law gives $T_c \sim 1.30$. Similarly, Sung and Chandler found a direct value $T_c = 1.35$, while fitting coexistence data for $0.85 \leqslant T \leqslant 1.15$ with a scaling law a lower T_c (1.31) was obtained. We also performed such an experiment with our EOS coexistence data for $T \leqslant 1.15$, using critical exponents from the literature, ranging from $\beta = 0.32$ (Smit) to $\beta = 0.355$ (Adams), and the critical temperature was in this case estimated between 1.29 ($\beta = 0.32$) and 1.32 ($\beta = 0.355$).

We can, therefore, conclude that our values of the critical point, especially the QGE-B one, are about the most reliable for the '*NVT* Lennard-Jones' fluid, where

Downloaded By: [EBSCOHost EJS Content Distribution] At: 14:09 25 March 2008

Table 8. Estimates of the critical point of the Lennard-Jones fluid from different sources, based on molecular dynamics (MD) or Monte Carlo (MC) simulations in different ensembles [NVT, NpT, μVT and Gibbs ensemble (GE)], along with results of several integral equations (Percus–Yevick (PY, II) and optimized cluster theory (OCT)). The first group ('NVT' data) consists of direct estimates from EOS or Maxwell constructions based on simulation data along isotherms. The values of the second group ('Scaling law') were obtained by fitting the available coexistence points with a scaling law for the density with critical exponent β.

			'NVT' data			'Scaling law'			
Source	Reference	Method	T_c	ρ_{N_c}	p_c	T_c	ρ_{N_c}	p_c	β
QGE-A		NVT EOS	1.350	0.337	0.149				
QGE-B		NVT EOS	1.346	0.346	0.147				
LV (1969)	[44]	NVT MC EOS (7)	1.37	0.31	0.14				
LV (1969)	[44]	NVT MC EOS (11)	1.36	0.33	0.16				
V (1967)	[38]	NVT MD+ PYII	1.34(2)	0.34(2)	0.15(2)				
VL (1967)	[43]	PY, II-Vir	1.36(4)	0.36(3)	0.15(1)				
VL (1967)	[43]	PY, II-O.Z.	1.33(3)	0.33(4)	0.15(2)				
SC (1974)	[37]	OCT	1.348	0.349	0.148	1.31(1)	—	—	0.33
N (1979)	[5]	imposed	1.35	0.35	0.14				
A (1979)	[36]	μVT MC	1.33(2)	—	—	1.30(2)	0.33(2)	0.13(2)	0.355
KN (1994)	[7]	NVT EOS	1.340	0.311	0.141				
M (1996)	[8]	imposed	1.328	0.311	0.135				
P (1987)	[40]	GE MC				1.32	0.31(2)	—	—
S (1992)	[24]	GE MC				1.316(6)	0.304(6)	—	0.32
L (1992)	[39]	NpT MD+ test				1.310	0.314	—	1/3
J (1993)	[4]	imposed				1.313	0.310	—	
ST (1996)	[6]	imposed				1.313	0.310	0.1299	

large density fluctuations are suppressed. We can also illustrate this fact by comparing for example the pressure isotherms in the vicinity of the critical point as predicted by the QGE and MBWR-1 equations, where for the latter the critical point was imposed to be the one obtained from GE and NpT data [4], see table 8. In figure 8 we see that the QGE-B isotherm (on this scale identical to the QGE-A prediction) accurately describes the NVT simulation data of Johnson *et al.* and Sun and Teja, while the MBWR-1 predictions around $\rho_N \sim 0.4$ are systematically too high, as the imposed critical point does not match the NVT data in the critical point region.

Finally, we note that the critical point for the truncated and shifted LJ potental (i.e. without the truncation and shift corrections) is $T_c = 1.288$ and $\rho_{N_c} = 0.348$ for QGE-A and $T_c = 1.284$, $\rho_{N_c} = 0.361$ for QGE-B.

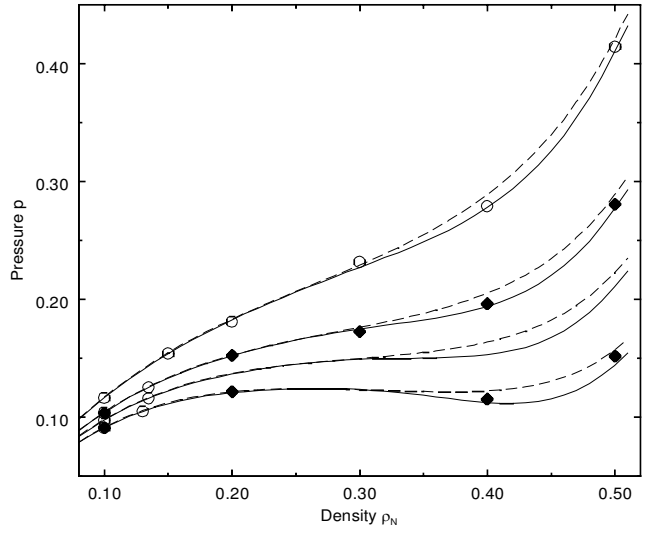

Figure 8. Experimental isotherms (from top to bottom $T = 1.5$, 1.4, 1.35 and 1.3) in the vicinity of the critical point, using data from Johnson *et al.* (◆) and Sun and Teja (○), and EOS predictions: QGE-B (——) and MBWR-1 (– – –).

7. Conclusions

In this article we showed how to use in a simple way the QGE theory at the Gamma level for the potential energy fluctuations to obtain a general equation of state for fluids. Introducing a simple perturbation term, we defined the perturbed confined Gamma state that, in combination with the knowledge of a set of properties (the input parameters) along a single isotherm, provided an accurate equation of state over a wide temperature-density range, for both the discrete density (DD) and continuous density (CD) approaches.

It is remarkable that the DD and CD QGE equations of state, parametrized in the smaller temperature range (dQGE-B and QGE-B) are very close to the ones para-

Downloaded By: [EBSCOHost EJS Content Distribution] At: 14:09 25 March 2008

metrized in the whole temperature range (dQGE-A and QGE-A). Hence the former can be used for extrapolations even much beyond their parametrization range.

It should be noted that the DD and CD equations can also reproduce with high accuracy data which were not used for the parametrization, like the heat capacity and, for the CD equations, the pressure. This clearly shows that the perturbed confined Gamma state, with the perturbation term given by equation (39), is a very good model for the Lennard-Jones fluid at every density, and confirms our previous results that the Gamma statistical state for the potential energy fluctuations can be used as a general theoretical model. For the Lennard-Jones fluid the use of the simple first order perturbation term is really necessary only if high accuracy over a very large temperature range is required; for a smaller temperature range a pure confined Gamma state is also accurate.

We compared the DD and CD QGE equations of state with three of the currently most successful equations of state for the Lennard-Jones fluid, the modified Benedict–Webb–Rubin (MBWR), the Kolafa–Nezbeda (KN) and Mecke *et al.* (VDW) equations. For the energy the data showed that the CD equations are more accurate than the MBWR equations, and comparable to the KN and VDW equations inside the parametrization range which they have in common. The CD equations were parametrized only on energy data, except at the reference isotherm, where pressure data were also used. Hence for the pressure they are less accurate than the other equations which were parametrized using both energy and pressure data, but still they can provide a rather accurate description of the pressure. The DD equations, which were parametrized using energy and pressure data, can reproduce both energy and pressure more accurately than the MBWR equations, and are at least comparable to the KN and VDW equations, again inside the parametrization range which they have in common. Very significantly, the DD as well as the CD equations provide accurate extrapolations much beyond their parametrization range, while the MBWR equations become rather incorrect outside their parametrization range.

It is also very interesting that the coexistence line obtained by the CD QGE equations is very similar to the one obtained by the MBWR equations, except for the critical point region, where a small deviation is observed. As shown in the results section this is probably due to the fact that in the MBWR equations of state the critical point was constrained to the critical temperature and density obtained from NpT and Gibbs ensemble MC simulations. In the QGE equations, we did not impose any predetermined critical point and the critical temperature and density found are in excellent agreement with the estimates obtained by NVT simulations or integral equations. Also the estimates from the KN equation are very close. This strongly suggests that the QGE equations of state, parametrized using NVT MD data, provide a better estimate of the true critical point of an NVT LJ fluid. The small discrepancy from the NpT and Gibbs ensemble estimates could in principle be due to the finite size effect, which is likely to influence the fluctuations of the system in the critical point region, as already pointed out by other authors. However, from our results it seems that the greater part of this difference is connected with the use of the macroscopic scaling law for the density.

It seems clear from all the results that an equation of state based on a not too simple physical theory can really provide an improved description of the fluid thermodynamics. On the one hand, it is possible to extrapolate to unknown state points, and on the other hand, the fact that the EOS describes the behaviour of a coherent physical model ensures that the detailed knowledge from the EOS is able to give a deeper insight into the fluid physics.

Future work will concern the application of the theoretical model described in this article to obtain equations of state for real fluids, the development of methods for the calculation of high order energy moments and energy-virial correlations from a molecular model potential, and the derivation of possible simple physical models to obtain the isotherm input properties with the use of a more reduced data set, especially for systems where no reliable model potential is available. We will also explore other kinds of models based on the QGE theory to obtain equations of state and possible simplifications of the present EOS. Finally, attention will be given to the technical aspects of the parametrization procedure that can be improved using more physical information and better numerical procedures (simulations and fitting algorithms).

We greatly appreciate the CPU time provided by CASPUR. We would also like to thank Danilo Roccatano for implementing the isothermal coupling into GROMACS and analysing part of the molecular dynamics simulations. Part of this research was financially supported by the Training and Mobility of Researchers programme of the European Union.

References

[1] Reid, R. C., Prausnitz, J. M., and Poling, B. E., 1987, *The Properties of Gases and Liquids*, 4th Edn (New York: McGraw-Hill).

[2] Reynolds, W. C., 1979, *Thermodynamic Properties in SI* (Stanford: Dept. of Mechanical Engineering, Stanford University).

Downloaded By: [EBSCOHost EJS Content Distribution] At: 14:09 25 March 2008

[3] Angus, S., Armstrong, B., and de Reuck, K. M., 1976, *Methane*, Vol. 5, *International Thermodynamic Tables of the Fluid State* (Oxford: Pergamon Press).

[4] Johnson, J. K., Zollweg, J. A., and Gubbins, K. E., 1993, *Molec. Phys.*, **78,** 591.

[5] Nicolas, J. J., Gubbins, K. E., Streett, W. B., and Tildesley, D. J., 1979, *Molec. Phys.*, **37,** 1429.

[6] Sun, T., and Teja, A. S., 1996, *J. phys. Chem.*, **100,** 17 365.

[7] Kolafa, J., and Nezbeda, I., 1994, *Fluid Phase Equil.*, **100,** 1.

[8] Mecke, M., Mueller, J. W. A., Vrabec, J., Fischer, J., Span, R., and Wagner, W., 1996, *Int. J. Thermophys.*, **17,** 391.

[9] Smith, W. R., 1973. *Specialist Periodical Reports, Statistical Mechanics*, Vol. 1, edited by K. Singer (London: Chemical Society).

[10] Amadei, A., Apol, M. E. F., and Berendsen, H. J. C., 1998, *J. chem. Phys.*, **109,** 3004.

[11] Amadei, A., Apol, M. E. F., and Berendsen, H. J. C., 1997, *J. chem. Phys.*, **106,** 1893.

[12] Apol, M. E. F., Amadei, A., and Berendsen, H. J. C., 1998, *J. chem. Phys.*, **109,** 3017.

[13] Apol, M. E. F., Amadei, A., and Berendsen, H. J. C., 1996, *J. chem. Phys.*, **104,** 6665.

[14] M. E. F. Apol, 1997, PhD thesis, Rijksuniversiteit Groningen, The Netherlands.

[15] Stuart, A., and Ord, J. K., 1987, *Kendall's Advanced Theory of Statistics*, Vol. 1, 5th Edn (London: Griffin).

[16] Johnson, N. I., Kotz, S., and Kemp, A. W., 1992, *Univariate Discrete Distributions*, 2nd Edn (New York: Wiley).

[17] Patel, J. K., Kapadia, C. H., and Owen, D. B., 1976, *Handbook of Statistical Distributions* (New York: Marcel Dekker).

[18] Amadei, A., Apol, M. E. F., Di Nola, A., and Berendsen, H. J. C., 1996, *J. chem. Phys.*, **104,** 1560.

[19] Baker Jr, G. A., 1975, *Essentials of Padé Approximants* (New York: Academic Press).

[20] Baker Jr, G. A., and Gammel, J. L. (eds), 1970, *The Padé Approximant in Theoretical Physics* (New York: Academic Press).

[21] Landau, L. D., and Lifshitz, E. M., 1980, *Statistical Physics. Part 1*, Vol. 5, *Course of Theoretical Physics*, 3rd Edn (Oxford: Pergamon Press).

[22] Carnahan, N. F., and Starling, K. E., 1969, *J. chem. Phys.*, **51,** 635.

[23] Roccatano, D., Amadei, A., Apol, M. E. F., Di Nola, A., and Berendsen, H. J. C., 1998, *J. chem. Phys.*, **109,** 6358.

[24] Smit, B., 1992, *J. chem. Phys.*, **96,** 8639.

[25] Allen, M. P., and Tildesly, D. J., 1989, *Computer Simulation of Liquids* (Oxford: Oxford University Press).

[26] van der Spoel, D., van Buuren, A. R., Apol, E., Meulenhoff, P. J., Tieleman, D. P., Sijbers, A. L. T. M., van Drunen, R., and Berendsen, H. J. C., 1997, *Gromacs User Manual, Version 1.51*, (Nijenborgh 4, 9747 AG Groningen, The Netherlands), Internet: http://rugmd0.chem.rug.nl/~gmx.

[27] Evans, D. J., and Morris, G. P., 1984, *Comput. Phys. Rep.*, **1,** 297.

[28] Brown, D., and Clarke, J. H. R., 1984, *Molec. Phys.*, **51,** 1243.

[29] Evans, D. J., and Morris, G. P., 1983, *Phys. Lett.* A, **98,** 433.

[30] Straatsma, T. P., Berendsen, H. J. C., and Stam, A. J., 1986, *Molec. Phys.*, **57,** 89.

[31] Miyano, Y., 1993, *Fluid Phase Equil.*, **85,** 71.

[32] McQuarrie, D. A., 1976, *Statistical Mechanics* (New York: Harper & Row).

[33] Hansen, J. P., and McDonald, I. R., 1986, *Theory of Simple Liquids*, 2nd Edn (London: Academic Press).

[34] Hansen, J. P., and Verlet, L., 1969, *Phys. Rev.*, **184,** 151.

[35] Adams, D. J., 1976, *Molec. Phys.*, **32,** 647.

[36] Adams, D. J., 1979, *Molec. Phys.*, **37,** 211.

[37] Sung, S. H., and Chandler, D., 1974, *Phys. Rev.* A, **9,** 1688.

[38] Verlet, L., 1967, *Phys. Rev.*, **159,** 98.

[39] Lotfi, A., Vrabec, J., and Fischer, J., 1992, *Molec. Phys.*, **76,** 1319.

[40] Panagiotopoulos, A. Z., 1987, *Molec. Phys.*, **61,** 813.

[41] Panagiotopoulos, A. Z., Quirke, N., Stapleton, M., and Tildesley, D., 1989, *Molec. Phys.*, **63,** 527.

[42] Smit, B., and Frenkel, D., 1989, *Molec. Phys.*, **68,** 951.

[43] Verlet, L., and Levesque, D., 1967, *Physica*, **36,** 254.

[44] Levesque, D., and Verlet, L., 1969, *Phys. Rev.*, **182,** 307.

[45] Barker, J. A., and Henderson, D., 1976, *Rev. mod. Phys.*, **48,** 587.

[46] Rowlinson, J., and Swinton, F., 1982, *Liquids and Liquid Mixtures*, 3rd Edn (London: Butterworths).

[47] Smit, B., de Smedt, P., and Frenkel, D., 1989, *Molec. Phys.*, **68,** 931.